

Style Definition: Default Paragraph Font

The multi-decadallong-term hazard cascade of an unprecedented wildfire in a tropical mountain wildfireecosystem

William Veness¹, Martha Day¹, Anthony C. Ross¹, Yazidhi Bamutaze², Jiayuan Han¹, Douglas Mulangwa^{3,4}, Andrew Mwesigwa⁴, Emmanuel Ntale⁵, Callist Tindimugaya⁴, Brian Guma⁴, Elisabeth Stephens^{3,6}, Wouter Buytaert¹

¹Department of Civil and Environmental Engineering, Imperial College London, London, SW7 2BB, UK

²Department of Geography, Geo-Informatics and Climatic Sciences, Makerere University, Kampala, Uganda

³Department of Meteorology, University of Reading, Reading, RG6 6BB, UK

⁴Ministry of Water and Environment, Kampala, Uganda

⁵Uganda Red Cross Society, Kampala, Uganda

⁶Red Cross Red Crescent Climate Centre, The Hague, The Netherlands

Correspondence to: William Veness (williamaveness@gmail.com)

Abstract. Climate change is driving wildfires to higher elevations, yet the hazard cascades that follow the emergent burning of pristine tropical mountain ecosystems remain largely unexplored. Here, we analyse the long-term cascade following a February 2012 wildfire that burned 31 km² of forest and wetland in Uganda's Rwenzori Mountains National Park-, including sections above 3800 m elevation with no major fire history in 12,000 years. Combining remote sensing, humanitarian records, field surveys, and interviews, we document ten major floods since 2012, including two debris floods that required large-scale humanitarian responses. Post-fire increases in erosion and mass movement have widened the River Nyamwamba sevenfold since 2012, breaching copper-cobalt mine tailings and mobilising an estimated 744,000 tonnes of waste into the river. Slow vegetation recovery at high altitudes and positive feedbacks between hazards have prolonged this high-risk state-, underseoring the susceptibility of tropical mountain ecosystems to long term post wildfire caseades. More monitoring and research are required to characterise key hazard interactions after tropical mountain fires, which can guide entry points for management seeking to mitigate future hazards. These findings point to an urgent need to understand where emergent tropical mountain fires can occur, how their impacts cascade downstream, and where early interventions can reduce risk.

Formatted: Highlight

1 Introduction

Climate and land-use changes are driving more frequent and intense wildfires across many tropical ecosystems worldwide (Ometto et al., 2022; UNEP, 2022; Wimberly et al., 2024; Obando-Cabrera et al., 2025). In tropical mountains, fires are burning at higher elevations (Mason et al., 2026; Xiao et al., 2022), which is exposing mature forests and wetlands that are not adapted to burning regimes. Tropical mountain forests cover 1.8 million km² globally (FAO & UNEP, 2020), and they provide the headwaters of major river systems such as the Nile, Amazon and Mekong to sustain the livelihoods of over 336 million people (Encalada et al., 2019).

Hazard cascades describe networks of interconnected hazard processes, where a primary event initiates a sequence of subsequent hazards through direct or indirect interactions (Gill and Malamud, 2016). Understanding cascade dynamics is essential for risk assessment, as the cumulative impacts of cascading hazards often exceed those of individual events in isolation (Gill and Malamud, 2016). Tropical mountains host multiple hazards, making them susceptible to multi-hazard cascades (Arango-Carmona et al., 2025). Intense convectional rainfall drives flash floods (Encalada et al., 2019), whilst high temperatures at lower elevations encourage the development of droughts, heatwaves and wildfires (Ometto et al., 2022). In addition, their steep gradients, deeply chemically weathered soils and unconsolidated glacial and fluvial deposits also favour landslides, debris flows and high rates of erosion (Arango-Carmona et al., 2025).

Multi-hazard cascades occur when two or more hazards interact through relationships characterised as *triggering*, *probability increasing*, or *catalysing/impeding* (Gill and Malamud, 2016). Triggering interactions are typically short-term, through directly sequenced hazard events such as a lightning storm triggering a wildfire. Probability increasing interactions occur when a hazard affects the environmental conditions in a way that increases the likelihood of subsequent hazards occurring. Wildfires are known to have probability-increasing relationships with a range of secondary hazards due to the destruction of vegetation and changes to the physical, structural and biochemical properties of soil (Vahedifard et al., 2024; Boyer et al., 2022). For instance, the probability of post-fire flash flooding is increased due to vegetation-loss reducing interception and thus increasing effective precipitation (Stoof et al., 2012). Whilst triggering and probability increasing hazard interactions describe how one hazard affects the occurrence of another hazard, catalysis/impedance relationships act upon other hazard interaction pairings. For example, the increased river discharge resulting from wildfires may catalyse ‘erosion-triggered-mass movements’ by adding energy and material to earth flows, and the loss of vegetation in a wildfire-affected area may impede the development of future wildfires triggered by human activities (Shakesby and Doerr, 2006). In practice, hazards often share multiple of these cascading interactions, and their relationships can evolve over time (Gill and Malamud, 2016).

64 1.1 Post-Wildfire Hazard Cascades

65 Despite their increasing risk, wildfire hazard cascades in tropical montane regions remain poorly understood. Most existing
66 research comes from temperate systems, where wildfires are known to amplify floods, accelerate erosion, and increase the
67 probability of landslides and debris flows by removing vegetation, altering soil properties and increasing surface runoff
68 (Belongia et al., 2023; Boyer et al., 2022; DeBano, 2000; Doerr et al., 2000; Guerriero et al., 2025; Jordan, 2016; Kemter et
69 al., 2021; Rengers et al., 2020; Swain et al., 2025; Vahedifard et al., 2024; McGuire et al., 2024).

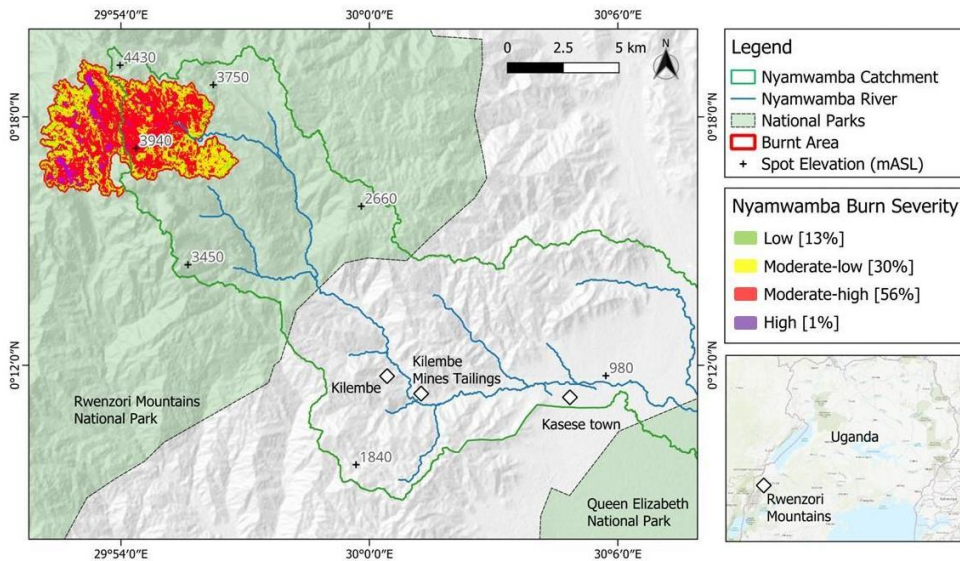
70
71 However, there are additional factors in tropical mountains that introduce a unique risk and complexity (Moazeni & Cerdà,
72 2024; Robinne et al., 2021). First, the fires impact upon an already diverse multi-hazard landscape with many existing hazard
73 interactions (Arango-Carmona et al., 2025; Ometto et al., 2022; Sandwell et al., 2005). Second, many higher-altitude
74 ecosystems within tropical mountains have no history of wildfire, such that mature climax vegetation and pristine wetlands
75 are burned with unpredictable consequences for hydrological processes and ecosystem services (Marengo et al., 2021; [Mason
76 et al., 2026](#); Pivello et al., 2021; UNEP, 2022). Third, a lack of wildfire history means vulnerable populations without lived
77 experience are exposed to new hazards (McCaffrey, 2004; Paton, 2003). Lastly, vegetation recovery at high altitudes is slow
78 due to cold conditions and the presence of vegetation that is not adapted to fire cycles, causing prolonged impacts (Kappelle
79 et al., 1996; Oliveras et al., 2014; Salinas et al., 2021). Given these differences, there is a need to better understand the long-
80 term cascade of tropical montane wildfires at the process level. This is especially true for multi-hazard risk management, as
81 identifying where hazards interact effectively highlights where those interactions can be proactively impeded (AghaKouchak
82 et al., 2018, Aghakouchak et al., 2020; Vahedifard et al., 2024).

83 1.2 Rwenzori Mountains National Park 2012 Wildfire

84 The February 2012 wildfire in Uganda's Rwenzori Mountains National Park burned 31 km² of pristine, uninhabited tropical
85 mountain forest and wetlands (Fig. 1) during a brief meteorological drought measuring -3.5 in a 1-month Standardised
86 Precipitation Index (Appendix A). [The fireThe ecosystem was mature – the fire was the first to affect elevations exceeding
87 3800 m above sea level in the Rwenzori Mountains for at least 12,000 years \(Mason et al., 2026\).](#)

88
89 [The wildfire](#) was followed by unprecedented debris flooding in May 2013 that displaced more than 25,000 people, caused 13
90 deaths and over USD \$4 million in damages (Delforge et al., 2025). Local rainfall records suggested only a 6.6-year return
91 interval (6-hour duration), indicating that post-fire landscape changes drove the disaster (Jacobs et al., 2016). We present
92 evidence that, more than a decade later, the Nyamwamba catchment continues to experience flooding, debris floods, mass
93 movements, erosion and water pollution [at an elevated level](#) due to fire-induced environmental changes. Because the wildfire
94 occurred in a protected area with no burn history and little subsequent intervention ([Mason et al., 2026](#); Norville, 2024), it
95 provides an unparalleled case for this study to characterise the long-term multi-hazard cascade of a tropical mountain wildfire.

96



97

98

99

100

101

Figure 1: The River Nyamwamba catchment and the delineated wildfire burn area within the Rwenzori Mountains, Uganda. Differenced Normalised Burn Ratio (dNBR) between pre- and post-fire Landsat-7 images were used to delineate the extent and burn severity of the February 2012 wildfire. Severity is classified according to the United States Geological Survey's guide (Key & Benson, 2006).

102

1.3 The Study Region

103

104

105

106

107

108

109

110

111

112

113

The Rwenzori Mountains are an uplifted metamorphic basement block, with hard, crystalline basement geology creating steep gradients and river profiles that climb to a maximum elevation of 5,109 m (UNESCO, 2012). It is the third largest glaciated region in Africa (Hinzmann et al., 2024), with abundant quaternary deposits of unconsolidated glacial and fluvial sediment in its valleys (UNESCO, 2012; Ring, 2008). The Rwenzori Mountains National Park is a UNESCO World Heritage Site dedicated to the protection of biodiverse and unique montane flora, classified into five distinct eco-zones (UNESCO, 2012): tropical mixed broadleaf montane rainforest (<2600 m altitude); bamboo forest (2600-3000 m); an ericaceous zone characterised by dense giant heather trees, giant senecios and giant Lobelia (3000-3800 m); afro-alpine moorland and bogs (3800 – 4400 m); and the rock, snowfield and glacier zone (>4400 m).

Higher altitudes within the equatorial mountain range have an annual precipitation of 2500 mm, with two wet seasons (March-May and September-December) where monthly precipitation values exceed 375 mm (UNESCO, 2012). The River

Formatted: Justified

114 Nyamwamba is a major river in the southern part of the Rwenzori Mountains that transports water to its delta with Lake George
115 within the Queen Elizabeth National Park area (Fig. 1).

116 **1.4 Study Scope**

117 This study characterizes the multi-decadal hazard cascade profile of the Nyamwamba River catchment following a 2012
118 wildfire that burned 31 km² of pristine tropical mountain forest and wetland in Uganda's Rwenzori Mountains National Park
119 and interprets the implications for regional risk management and broader lessons for tropical montane environments globally.
120 Through an integrated mixed-methods approach combining remote sensing analysis, humanitarian records, field surveys, and
121 semi-structured interviews, we document the long-term interactions between wildfire, flooding, erosion, landslides, and
122 pollution over a 12-year period (2012-2024). The study identifies key hazard interactions using Gill and Malamud's (2016)
123 framework, evaluates entry points for management interventions to mitigate future hazards in fire-sensitive tropical mountain
124 ecosystems, and derives take-aways for the governance and resilience of tropical montane regions facing emerging fire-driven
125 risks.

126 **2 Methods**

127 We adopted a mixed methods approach to evidence changes in multi-hazard processes and risk, combining remote sensing,
128 humanitarian data, field observations and key informant interviews. Cross-validation across methods enabled an abductive
129 approach (Saunders et al., 2016), where emerging insights, such as interview reports of erosion, informed subsequent lines of
130 data collection and analysis.

131 **2.1 Remote Sensing and GIS**

132 **2.1.1 Data Acquisition and Pre-Processing**

133 Annual Landsat-7 (2006 – 2012) and Landsat-8 (2013-2024) Level-2 surface reflectance images at 30m resolution were
134 downloaded from the United States Geological Survey (USGS) earth explorer and gap corrected, cropped and cloud masked
135 for analysis (Congedo, 2021). For each year, the earliest post-January 1 image with <10% cloud cover was selected. High-
136 resolution Google Earth Pro imagery was used to measure river width, while Maxar mosaics visualised mine tailings erosion
137 (Maxar Technologies, 2025a; Maxar Technologies, 2025b).

138 **2.1.2 Burn Severity Classification**

139 Burned area was delineated using the Normalised Burn Ratio (NBR), which combines Landsat 7 near-infrared (Band 4) and
140 shortwave-infrared (Band 7) reflectance (Key & Benson, 2006) to map and quantify the severity of a fire's impact on vegetation

141 and soil. The difference between pre- (9 January 2012) and post-fire (28 March 2012) NBR values (dNBR) provided a relative
142 severity index following USGS protocols (Key & Benson, 2006).

143 **2.1.3 River Channel Bank Erosion Analysis**

144 Supervised minimum-distance land-cover classifications were applied to annual Landsat images from 2006 – 2024, using fixed
145 ground control points for five classes: eroded river channel, tailings, oxidised iron, vegetation, and agriculture (Congedo,
146 2021). Each image was clipped to the Nyamwamba channel, and classified areas were validated against Google Earth area
147 estimates with a relative error of 3.84%. Cumulative lateral riverbank eroded area was plotted over time, with classification
148 maps from 2006 and 2021 shown for comparison. River width was delineated in 2010, 2014, 2018, and 2021, at 1 km intervals
149 along 20 km of channel between Kilembe town and Lake George.

150 **2.1.4 Tailings Erosion**

151 Erosion of the Kilembe Mines tailings was assessed using Maxar mosaics from March 2006 and April 2023, with the 33,000
152 m² eroded footprint delineated manually. Field measurements in July 2024 using a laser rangefinder provided site dimensions,
153 from which eroded volumes were calculated (see Appendix B).

154 **2.2 Humanitarian Data Analysis**

155 Historic flood events in the Nyamwamba catchment since 2000 were compiled from multiple open sources: the Emergency
156 Events Database (Delforge et al., 2025), the Sendai DesInventar database (DesInventar, 2025), grey literature in ReliefWeb,
157 and a systematic keyword search (“Kasese” OR “Kilembe” AND “flood”) across Google, Google Scholar, and Google News
158 (Google News, 2025). While recent years benefit from expanded monitoring and reporting, the inclusion of diverse sources
159 provided confidence that all major flood events since 2000 were captured by the search.

160 **2.3 Interviews**

161 We conducted twelve in-person semi-structured interviews during field visits in 2023 and 2024, following ethical clearance.
162 Participants were identified through project partners in Kasese District, with snowball sampling to access other stakeholder
163 groups. They included 2 representatives from the Ministry of Water [M – code used to reference in the results], 2 local
164 government officials [G], 1 wildlife authority employee [W], 1 non-governmental organisation worker [N], 2 local industry
165 workers [I], 1 farmer [F], and 3 community residents [R].

166
167 Interviews followed a lightly structured topic guide covering hazard processes and causes, changing risk, existing management,
168 and potential alternatives, while remaining flexible to emergent themes (Creswell, 2009; Galletta, 2013; Mojtahed et al., 2014).
169 A full guide is provided in Appendix C. Interviews lasted 30 – 120 minutes, were audio-recorded, transcribed, and coded
170 inductively over two rounds of review, with related codes grouped into interpretive themes (Patton, 2014; Saldana, 2021).

171 While themes are not presented directly, this analysis informed interpretation of hazard processes, impacts, and management
172 options.

173 **2.4 Photographs**

174 Historic photographs of the vegetation pre- and immediately post-wildfire were taken by project partners with permission for
175 research use. Photographs in Appendices E – J were taken by the study authors during a July 2024 site visit.

176 **2.5 Cascade Visualisation**

177 Processes identified through the above methods were integrated into a conceptual diagram of the wildfire’s multi-hazard
178 cascade (Patton, 2014), following Gill & Malamud’s (2016) framework for hazard interaction types. Evidence underlying each
179 connection is documented throughout the Results and summarised in Table D1 (Appendix D).

180 **3 Results**

181 We present the multi-hazard cascade caused by the 2012 Rwenzori National Park wildfire (Fig. 2). The following sections
182 describe each of the hazards involved and the interactions they drive, based on evidence from our mixed methods. Results are
183 structured by hazard type: wildfire (Sect. 3.1), flooding (3.2), landslides (3.3), erosion (3.4), and pollution (3.5). Identified
184 interactions highlight opportunities where management interventions can impede the cascade, for which we discuss practical
185 solutions at the local and global scales in Sect. 4 (Discussion). The hazard definitions follow the Hazard Information Profiles
186 (UNDRR, 2025) and are clarified in Table D1 (Appendix D). Importantly, here landslides refer to gravitational mass
187 movements directly connected to the river system as shown in Figures I1 and I2 (Appendix I).

188
189
190

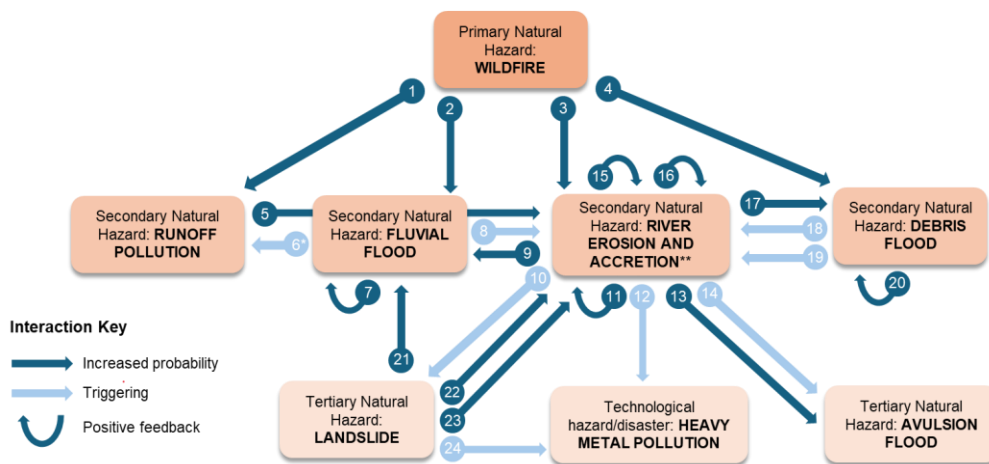


Figure 2: Conceptual model of the multi-hazard cascade following the Rwenzori National Park wildfire in February 2012. Interactions between hazards are classified as being (i) triggering, or (ii) probability increasing, following Gill and Malam ud's (2016) framework, and (iii) positive feedbacks have been identified. There are numerous catalysing/impeding relationships in this context, which we omit from the visualisation for simplicity but describe key examples in the analysis text. Table 1 describes each of the interactions shown.

*Interaction (6) also applies for debris floods and avulsion floods as the driving hazard (Table 1), but they are grouped for simplicity in the visualisation.

**River channel erosion and accretion of eroded sediment are treated as one hazard in line with UNDRR's Hazard Information Profiles (HIPs), with continuously interacting processes and positive feedbacks (15, 16) along the river's reach (UNDRR, 2025).

Table 1: Description of the hazard cascade interactions in Fig. 2. The study evidence for each interaction is explained in the text and summarised in Table D2 (Appendix D).

Driving Hazard	Description of Interaction	Affected Hazard
Wildfire	1 Wildfire generated ash & exposed soils to surface runoff	Runoff Pollution
	2 Burning increased runoff & river discharge, causing higher peak flows	Fluvial Floods
	3 The higher peak river discharge has increased the river's erosive power	Erosion and Accretion
	4 The higher peak river discharge has increased its transport competence	Debris Floods
Runoff Pollution	5 Increased sediment loads, more material available for accretion	Erosion and Accretion
Fluvial Floods	6 Floodwaters (fluvial, *avulsion and debris floods) transport contaminants across the landscape	Runoff Pollution
	7 Each flood damages natural banks & flood defences	Fluvial Floods
	8 Higher flow velocities & turbulence during floods increase erosion	Erosion and Accretion
River Channel Erosion	9 Eroded material fills the channel, reducing its discharge capacity	Fluvial Floods
	10 Lateral erosion undercuts & destabilises hillslopes	Landslides

and Accretion	11	Lateral erosion exposes bare riverbanks to further erosion	Erosion and Accretion
	12	Direct erosion inputs Co-Cu Kilembe Mines solid tailings into the river	Heavy Metal Pollution
	13	Higher erosion rates have increased channel-switching events	Avulsion Floods
	14	Eroded sediment deposits in channel bars, diverting flow to banks	Avulsion Floods
	15	Sediment deposition narrows channel increasing erosive potential	Erosion and Accretion
	16	Eroded sediment accretes in the channel, diverting flow to erode riverbanks	Erosion and Accretion
	17	Erosion generates additional sediment for debris flood formation	Debris Floods
Debris Floods	18	Debris floods have a high erosive power	Erosion and Accretion
	19	Mobilized sediment deposits in channel, diverting flow to erode riverbanks	Erosion and Accretion
	20	Debris floods damage natural banks & flood defences	Debris Floods
Landslides	21	Landslide talus fills the channel, reducing its discharge capacity	Fluvial Floods
	22	Increased sediment loads, more material available for accretion	Erosion and Accretion
	23	Landslides increase sediment loads, increasing erosion by abrasion	Erosion and Accretion
	24	Rotational slumping of tailings inputs waste to the river channel	Heavy Metal Pollution

203

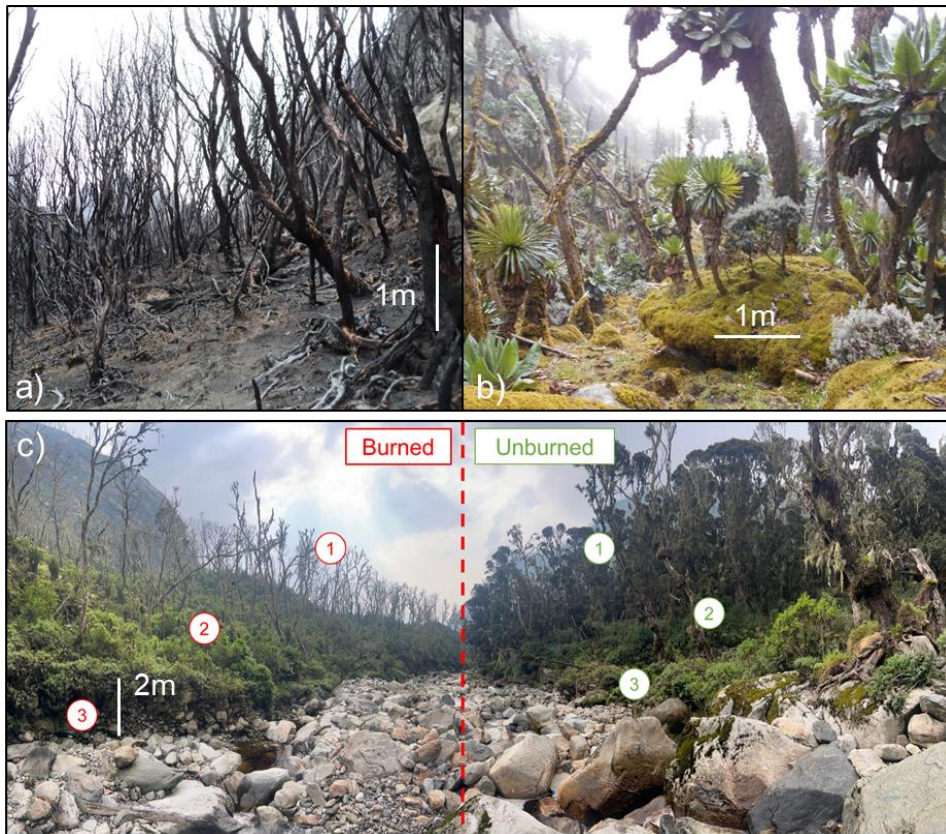
204 3.1 Wildfire

205 Remote sensing evidence shows a 30.75 km² burn area for the February 2012 wildfire (Fig. 1), with 87% of the area burned to
 206 a moderate or high severity. The fire occurred during a meteorological drought, with <0.2 mm of precipitation in the 4-weeks
 207 preceding the fire (Jacobs et al., 2016) and a one-month Standardised Precipitation Index measuring -3.5 for January 2012
 208 (Appendix A). The fire's cause of ignition is still unknown by the water and wildlife authorities [M1; M2; W1].

209

210 The fire burned between 3360 – 4400 m above sea level, burning climax 'heather zone' forest, "spongy" [R1] Afroalpine
 211 moorland, and methane-rich bogs [M1+; aH] with no recorded history of wildfires- (Fig. 3a; [Mason et al., 2026](#); UNEP, 2022).
 212 Photographs from March 2012 show indicators of high burn severity (Fig. 3b), while images from July 2024, twelve years
 213 later, reveal regrowth limited to a maximum of 2.5 m, with the upper canopy still vacant (Fig. 3c). These slow growth rates
 214 and an observed scarcity of heather in the regrowth succession indicate that natural recovery will require several decades
 215 (Wesche, Miehe and Kaeppli, 2000).

216



#	Attribute in c)	Burned	Unburned
1	Upper canopy	Dead ericaceous trees, vacant canopy	Mature ericaceous canopy
2	Lower canopy	Regrowth up to 2.5 m, heather scarce	Mature, dense vegetation
3	Riverbanks	Steep, unvegetated banks of exposed and unconsolidated glacial till	Sloped banks and coarse material anchored by vegetation

Formatted Table

217
218
219
220
221
222
223

Figure 3: a) burned ericaceous 'heather zone' vegetation 1-month after the wildfire in March 2012; b) Mature Afroalpine moorland vegetation prior to the wildfire (March 2011); c) upper course of the River Nyamwamba at 3380 m elevation in July 2024, where the river had acted as a firebreak to provide direct comparison between unburned and recovering burned sections of the ericaceous forest. Scale bars correspond to the tree trunk in 3a, the boulder in 3b and the riverbank in 3c. The associated table describes the ecological properties of the burned and unburned areas.

224 *Wildfire-driven Interactions*

225 The wildfire has unidirectional probability-increasing interactions with four secondary hazards. First, burning of soils and
226 vegetation cover increased surface erosion and runoff to river channels, raising turbidity, carrying ash and peat, and introducing
227 biological contaminants. Respondents recalled a strong smell “like methane” after the fire [M1; M2; R1; G1], highlighting
228 wildfire-driven runoff pollution (#1). Second, reduced interception and infiltration capacity increased peak discharges at
229 shorter lag times, driving a marked rise in fluvial flooding (#2; Sect. 3.2). Riverbank erosion has also accelerated due to higher
230 discharges and loss of root cohesion (#3; Sect. 3.4), which, together with higher peak flows after the wildfire, enhanced the
231 conditions for debris flood formation due to greater sediment supply [M1; R1] (#4, #17). These interactions (#1 - 4) are
232 unidirectional because none of the secondary or tertiary hazards have resulted in further occurrence of wildfires in the
233 catchment.

234

235 Additional relationships where the wildfire has catalysed other hazard interactions are numerous, but evidence for these cannot
236 fully be established without intensive monitoring and field experimentation. Based on hydrological theory, some interactions
237 catalysed by the wildfire’s effects would include:

238

- 239 • *River channel erosion-triggering-landslide (#10)*: increased discharge after the wildfire (Moody and Martin, 2001)
240 catalyses the generation of landslides caused by erosive undercutting from higher river erosion rates (Korup and
241 Schlunegger, 2007).
- 242 • *Landslide-increasing probability-river erosion (#23)*: increased discharge catalyses the contribution of landslides to
243 later erosion by transporting landslide talus and using the sediment as erosive tools for abrasion (Sklar and Dietrich,
244 2001)
- 245 • *Debris flood-triggering-river erosion (#18)*: increased discharge catalyses erosion during debris flood events by
246 increasing the erosive power of the flood (Stock and Dietrich, 2003)
- 247 • *Landslide-increasing probability-fluvial flood (#21)*: increased discharge increases the volume of water
248 accumulating in damming and bursting flood mechanisms after landslides (Costa and Schuster, 1987; Rudoy, 2002)
- 249
- 250
- 251

252

253 Although many of the other hazards in the cascade are responsible for additional catalysing relations, we only present examples
254 for the wildfire hazard in this study. This is to emphasise that the fire has not only increased the probability of four secondary
255 natural hazards at the start of the cascade, but it is also catalysing subsequent interactions between other hazards.

256 **3.2 Flooding**

257 All twelve respondents reported heightened flood risk in the Nyamwamba catchment. Five attributed this directly to changes
258 in hydrological processes caused by the 2012 wildfire [M1; M2; G1; G2; R1], while others cited land use change [N1; W1;

R3], climate change [N1; I2], or the discontinuation of dredging [I1; R2]. A government official explained that “*the burning is the reason we are now having the floods annually... we know how useful wetland vegetation is in controlling floods, releasing water slowly*” [G1]. Similarly, a local guide described the flood-buffering role of the alpine wetlands: “*the moss was like a big 1 m thick sponge, it soaked up all the rain... 20 or 30 km² of rock that was once boulders covered in moss is now bare*” [R1]. Table 2 documents ten flood events since 2012, all exceeding in intensity the two documented events during the preceding 12 years, with the 2013 and 2020 debris floods requiring international humanitarian appeals (Act Alliance, 2020; Delforge et al., 2025; Okiror, 2020).

Table 2: Timeline of flood events of the Nyamwamba River documented by humanitarian databases and grey literature since 2000. The dates of the two most intense debris flood events are highlighted bold.

Date	Area(s) Affected	Description & Impacts
1 st May 2001	Rukoki, Kilembe	1 death and 300 people affected by flooding in Kasese District (Delforge et al., 2025; DesInventar, 2025)
8 th September 2010	Rukoki, Ihandiro	A house, truck, pipeline and fields of crops destroyed by minor riverine flooding (Delforge et al., 2025).
<i>February 2012 – Wildfire burns 30.75 km² of the Rwenzori National Park</i>		
1st & 5th May 2013	Kilembe, Kasese District	Flooding and debris flooding in the Nyamwamba, Mubuku, Bulemba and Kitakena rivers displaced 25,445, with 13 deaths and US\$4,055,000 of damage (Delforge et al., 2025). Formal humanitarian response appeal of \$220,497 made by ACT Alliance (Act Alliance, 2013).
14 th May 2014	Kasese town	3,725 affected and 4 deaths in Kasese (DesInventar, 2025).
18 th June 2014	Kilembe	Flooded hospital and secondary school (Asimwe, 2014).
18 th April 2016	Kanamba, Kanaka, Kasese District	10,000 affected and an estimated \$3,428,000 of damage following flooding of the Nyamwamba, Sebwe and Mubuku rivers between 4 th – 18 th April (Delforge et al., 2025; DesInventar, 2025; Juma, 2016).
4 th July 2017	Kilembe	4 killed in the Kilembe Valley (DesInventar, 2025).
5th May 2020	Kasese District	173,000 people affected in 24,760 houses across Kasese and Bundibugyo Districts following flooding of major rivers (Delforge et al., 2025). Debris and fluvial flooding on the River Nyamwamba submerged the Kilembe Mines hospital, with over 1,200 people displaced in Kasese town (Act Alliance, 2020; Flood List News, 2020a, 2020b). Formal humanitarian appeal for assistance made by the Ugandan Red Cross to support the displaced (Okiror, 2020)
23 rd May 2021	Kilembe	3 deaths and 134 affected following flooding and landslides in Kilembe town (Delforge et al., 2025).
18 th May 2023	Kasese District	1,016 people affected, and 23 deaths recorded between 24 th April and 18 th May due to multiple floods of the Muhokya, Mubuku, Sebwe and Nyamwamba rivers (Delforge et al., 2025).
22 nd May 2024	Kilembe, Kasese town	Sudden change of river course during high flow. Debris floods, riverine flooding and mudslides in the Nyamwamba catchment displaced 5,389 people in Kasese town (New Vision, 2024).

Formatted Table

7 th September 2024	Kasese Town	2 deaths and extensive damage to key infrastructure including schools, roads, bridges and 120 houses. Change of course of river during high flows breached same location as the 22 nd May 2024 flood (ReliefWeb, 2024).
--------------------------------	-------------	--

269

270 The wildfire has increased the frequency and magnitude of fluvial flooding, but also introduced two new mechanisms of
 271 flooding, with gravity-driven debris floods and avulsion floods linked to increased mass movement (Sect. 3.3) and erosion
 272 (Sect. 3.4) in the catchment [M1; M2].

273 *Fluvial flooding*

274 Vegetation and soil loss following the wildfire reduced interception, infiltration, and water retention capacity, amplifying the
 275 river’s discharge response to rainfall. The fluvial flooding of unprecedented intensity on 5th May 2013 followed rainfall of
 276 only a 6.6-year estimated return period for a 6-hour event (Jacobs et al., 2016). Two respondents emphasise that a lack of lived
 277 experience prior to this first flood created additional vulnerability among affected communities: “2013 - that was when we
 278 were all surprised. I could not believe what I saw” [I1]; “we were not prepared because we had never experienced such
 279 magnitude” [M1]. Seven years later, an industrial worker recalled the 2020 event as “an 800 cumecs flood... higher than our
 280 professional hydrologist’s modelling of a 1000-year flood event” [I2].

281 *Debris flooding*

282 Two floods (2013 and 2020) included debris floods, confirmed in video footage and respondent testimony [M1; R1]. A water
 283 authority described “entire mahogany trees coming down as flood load” [M1], while a resident noted “moving rocks two times
 284 the size of a minibus” [R1]. Field photos (Appendix G) confirm extensive boulder deposition on the floodplain, and the river
 285 has since shifted from a pre-wildfire meandering form with vegetated banks to a braided morphology laden with coarse
 286 crystalline sediment (Appendix K).

287 *Avulsion flooding*

288 Elevated erosion rates and sediment deposition have heightened the risk of avulsions [M1; M2]. On 22nd May 2024, for
 289 example, the Nyamwamba breached its outer bank upstream of Kasese town, inundating Kiwa hot springs and displacing 5,389
 290 people [M1] (Table 2).

291 *Flood-driven Interactions*

292 High flows during fluvial and debris floods damage engineered flood defences, increasing their own probabilities of future
 293 breaches in self-perpetuating positive feedback (#7; #20; Appendix H). At the same time, their elevated velocities and
 294 turbulence generate shear stress and hydraulic action that trigger river erosion and accretion (#8; #18, #19). GIS analysis
 295 confirms that the years of greatest erosion (2013 and 2020) coincided with the largest debris flood events [M1; R1] (Sect. 3.4).

296 Fluvial, avulsion and debris floods transport contaminants across urban and agricultural landscapes, driving runoff pollution
297 (#6*; Appendix L). Additionally, debris floods deliver mobilized sediment directly into the river channel, promoting accretion
298 and progressively altering channel geometry over time (#19) [M1; M2; R1] (Figure 4).

299 3.3 Landslides

300 Landslides caused by lateral river erosion undercutting riverbanks and hillslopes (Jacobs et al., 2016) have accelerated since
301 the wildfire due to higher post-fire discharges and sediment loads [I1; M1; M2; R1]. In addition, the initial destruction and
302 exposure of formerly stable riverbanks during the wildfire and 2013 flood has worked to further increase the probability of
303 mass movement into the river [M1; G2]. Previously, graded banks of unconsolidated quaternary sediment were anchored by
304 climax vegetation. Now, vertical riverbanks are exposed to direct erosion and undercutting at sites throughout the river's long
305 profile. As one local government representative describes, "*when the floodwaters come down, they remove soil and grasses to*
306 *expose more boulders, and then you will have a landslide*" [G2]. This process is visible in Fig. 3c, where the riverbanks on
307 sections of the burned side are now steep, unvegetated banks of exposed and unconsolidated glacial till.

308 *Landslide-driven Interactions*

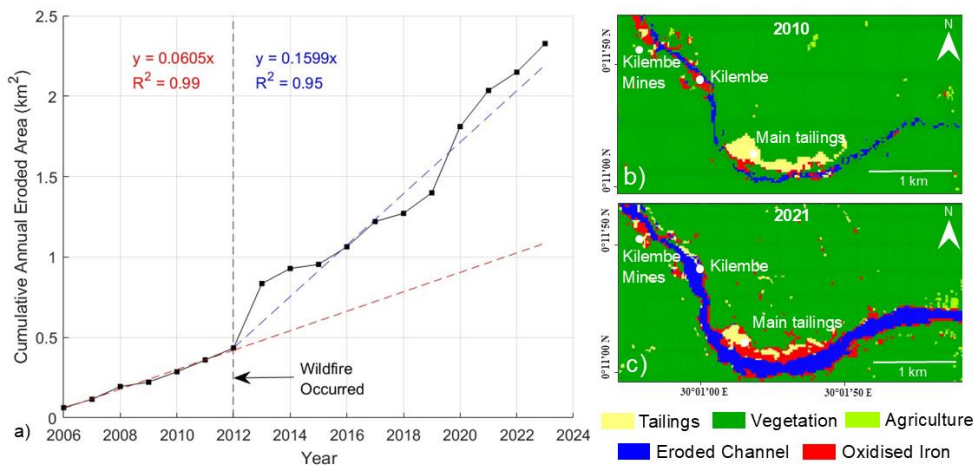
309 Landslides increase the probability of fluvial flooding by filling the channel with sediment and reducing the river's discharge
310 capacity (#21). Five respondents have also witnessed a mechanism of temporary landslide damming and bursting "*in the space*
311 *of a few minutes*" [M1] during high flow events, from which surges of sediment and discharge activate fluvial floods and debris
312 floods [G1; M1; M2; R1; W1]. As one resident recalls: "*suddenly, I heard a roar like a plane taking off at Entebbe Airport.*
313 *Two landslides cut off the river and created a dam behind it, then soon after there were entire trees pole vaulting over the*
314 *debris*" [R1].

315
316 Five respondents describe landslides as being in a positive feedback process with erosion (through reciprocal interactions #23,
317 #22 and #10), whereby landslides add load to the river, accelerating accretion and lateral erosion by diverting flow to the
318 riverbanks and trigger further landslides [R1; M1; M2; I1; G2]. Landslides also trigger heavy metal pollution through the
319 rotational slumping of solid Co-Cu tailings at Kilembe Mines into the River Nyamwamba (#24; Sect. 3.5).

320

321 3.4 River Channel Erosion and Accretion

322 The cumulative annual eroded river channel area (Fig. 4a) shows a sustained increase in the river's rate of erosion by a factor
323 of 2.64 following the 2012 wildfire, and the average middle-lower course channel width has increased sevenfold between 2010
324 – 2021, from 16.9 m to 123 m. Rapid erosion has destroyed agricultural land [M1; M2; G1; G2], residential property, and
325 critical road infrastructure [M1].



326
 327 **Figure 4: a) Annual cumulative eroded area in a 20 km mid-lower course section of the River Nyamwamba, calculated as the increase**
 328 **in eroded channel area between each year’s supervised classification; b) supervised classification of a February 2010 Landsat-7**
 329 **image; c) supervised classification of a February 2021 Landsat-8 image.**

330 *Erosion and Accretion-driven Interactions*

331 Since the wildfire, accelerated lateral river channel erosion has shifted the river channel closer to populated areas of Kasese
 332 town and eroded debris has filled the channel via deposition, reducing its discharge capacity. Together, these erosion and
 333 accretion processes increase the probability of urban flooding in Kasese town [R1; G1; G2; M2; I2; R3] (#9). Accretion also
 334 increases the probability of avulsion flooding, as exemplified by the May and September 2024 floods, by filling the channel
 335 with sediment bars that divert flow towards riverbanks [M1] (#13), whilst directly triggering avulsion floods when it breaks
 336 through unconsolidated banks [M1; M2] (#14). Contributions of sediment to the main Nyamwamba channel also increase the
 337 probability of debris floods [M1; R1] (#17).

338
 339 Erosional undercutting destabilises slopes and directly triggers landslides (#10), consistent with Jacobs et al.’s (2016) mapping
 340 of 14 bank-failure slides during the May 2013 multi-hazard event. This lateral undercutting and exposure of vertical riverbanks
 341 is also described by three respondents as putting erosion in self-perpetuating positive feedback, by increasing the probability
 342 of further erosion at exposed banks [G1, G2, M1] (#11).

343
 344 Erosion and accretion are also coupled through reciprocal feedback (#15, #16). Sediment deposition narrows the active channel
 345 cross-section, increasing the flow velocity and erosive potential (#15), driving further channel erosion. The eroded material

346 replenishes the sediment supply available for sediment deposition (#16), sustaining this cycle. Together, these dynamics place
347 erosion and accretion in a self-reinforcing feedback loop along the river’s reach.

348

349 Channel widening breached the Kilembe mine copper-cobalt tailings deposit in 2014 triggering heavy-metal pollution
350 downstream that now presents a major risk to public health (#12; Sect. 3.5).

351

352 **3.5 Pollution**

353 Immediately after the 2012 wildfire, community members reported increased turbidity and a smell “*like methane*” [M1] in the
354 river. This is still reported during high discharge twelve years later, which four respondents believe to be due to runoff (non-
355 point source) pollution through exposed bogs and organic-rich glacial sediments in the fire-affected and eroding upper
356 catchment [M1; M2; R1; G1] (#1).

357

358 Beyond this diffuse pollution, accelerated river erosion (#12) and landslides (#24) have inputted an estimated 744,000 tonnes
359 of a 15 Mt Kilembe Mines Co-Cu tailings deposit directly into the River Nyamwamba (mapped in Appendix K). Satellite
360 imagery and field photographs show erosional banks, slump scars and new channels within tailings areas, and evidence of acid
361 mine drainage from distinctive iron oxide precipitation (Fig. 3c; Appendix E). Elevated Co, Ni, Cu, Fe, Al, S, Zn, As, Cd and
362 Mn river contamination has previously been attributed to leaching of the Co-Cu mine (Abraham & Susan, 2017; Mwesigye et
363 al., 2016; Mwesigye & Lawrence, 2024; Mwongyera et al., 2014).

364

365 Five respondents identified this solid waste pollution as a major concern for public health [M2; W1; G1; G2; R1]. The river is
366 used by 38% of its adjacent population for drinking, and by many more indirectly through crop-irrigation and groundwater
367 abstraction (Abraham and Susan, 2017; Mukisa et al., 2020). In addition to waterborne risks, long-term contamination of arable
368 soils by deposited mine waste raises concern for food safety [M1; M2; G1; G2]. As one Ministry of Water official noted, “*in*
369 *Kasese District, their teeth are turning brown with yellow patches, and we have been told that many people in this region are*
370 *ailing with cancer*” [M2]. Local environmental managers also expressed concern for downstream ecosystems in Queen
371 Elizabeth National Park and Lake George, where protected flora and fauna may be affected by the pollution and vegetation
372 dieback observed in Kasese town [G2; M1, R1, W1].

373

374 *Pollution-driven Interactions*

375 Runoff pollution from the burned area transports elevated loads of fine sediment and contaminants into the river channel (#1)
376 [M1; M2; R1; G1]. This increased sediment supply promotes channel accretion as the excess sediment load settles into the
377 river channel (#5).

378 **4 Discussion: Implications for Management**

379 The intensity and persistence of the Rwenzori hazard cascade highlights how **emergent** wildfires in mature, fire-sensitive
380 mountain ecosystems can impose long-lasting risks on downstream communities. Recovery in these environments is slow, and
381 positive feedback mechanisms sustain elevated risk. By characterising hazard interactions in full, this study identifies entry
382 points for intervention as management approaches that systematically impede hazard interactions can help unravel cascades
383 (Gill and Malamud, 2016).

384
385 The principal way to impede this cascade is at the top (interactions #1-4), by promoting ecosystem recovery and attenuating
386 the elevated runoff and river discharge driving other hazards. In the Rwenzori, authorities implemented a mix of hard
387 engineering, community-centred and nature-based solutions in the lowlands which has saved lives (see Appendix M); however,
388 the prevailing approach to wildfire restoration has been to await natural recovery. This passivity missed a critical window to
389 implement soil stabilisation and runoff attenuation solutions such as mulching, contour felling and forest restoration
390 (Papaioannou et al., 2023; Robichaud et al., 2013; Scheper et al., 2021), and allowed lower canopy vegetation to establish
391 ahead of upper canopy tree species in the ericaceous zone (Fig. 3c). The challenge now is to develop recovery and discharge
392 attenuation solutions in a partially recovered ecosystem. Addressing this requires post-wildfire expert assessment to guide
393 restoration planning and build an evidence-base for financing solutions (Veness and Buytaert, 2025).

394
395 In the later stages of the Rwenzori cascade, erosion emerges as a key driver of multiple hazard interactions and positive
396 feedback processes. It has accelerated landslides, amplified debris floods, triggered flooding, and caused a major water
397 pollution hazard now requiring urgent investigation of its scale and health impacts. Stabilising riverbanks is a critical
398 intervention to mitigate erosion and therefore impede its cascading interactions. We recommend integrating existing dredging,
399 levee construction, and nature-based approaches to achieve this (Appendix M; MoWE, 2022). In particular, repositioning
400 coarse sediment to riverbanks can help protect eroding riverbanks, regrade unstable slopes, and create conditions for in-channel
401 vegetation to anchor finer sediments and restore soil, thus mimicking the stable, unburned riverbank morphology seen in Fig.
402 3c (Sanchez Fernandes et al., 2020). These measures are urgent in the mid-catchment to protect communities and limit further
403 mobilisation of solid mine waste, but also advisable in the upper catchment to reduce sediment generation and landslide risk.

404
405 The principle of mimicking natural processes to promote post-wildfire recovery has been successfully implemented elsewhere
406 (European Environment Agency, 2025). In New Mexico, Engineering With Nature (EWN) principles were implemented
407 following the 2011 Las Conchas Wildfire to implement low-tech hillslope and in-channel structures including mulch barriers,
408 contour-felled log debris, tree-check dams, and in-channel sediment grade-control features to stabilise slopes and reduce
409 downstream sediment transport (Haring et al., 2021). In Arizona, USA, following the 2019 Museum Fire, alluvial fan
410 restoration through regrading and rock sill installation has a predicted reduction in downstream sediment transport of 70%

411 (Schenk et al., 2025). Post-fire restoration following the 2020 Cameron Peak Fire in Colorado included post-assisted log
412 structures and beaver dam analogues to attenuate peak flows and promote sediment aggradation in burned headwater streams
413 to replicate the hydrological buffering functions of pre-fire riparian systems (Wheaton et al., 2019; CPRW, 2026; Nichter et
414 al., 2026). Whilst these represent a small selection of examples, the underlying principle of designing interventions to mimic
415 pre-disturbance geomorphological and hydrological processes offers a transferable blueprint for post-wildfire management in
416 significantly altered catchments like the Nyamwamba (Haring et al., 2021; Bombino et al., 2024).

417
418 Montane environments globally, especially those without a history of fire, require greater investment in monitoring and
419 research into post-wildfire hazard cascades (Arango Carmona et al. 2025; [Mason et al., 2026](#); Wimberly et al. 2024). The lack
420 of comparable case studies makes it difficult to determine whether the Rwenzori represents an outlier or part of a broader
421 emerging trend; however, the intensity of the Rwenzori cascade, following a burn area of just 31 km², is a signal to trigger
422 post-fire risk assessments at lower thresholds of burn area and severity when ~~thean emergent~~ fire occurs in a fire-sensitive
423 mountain ecosystem- ([Mason et al., 2026](#)). Expanding research in similar regions ~~withmay~~ help build an evidence base of
424 [comparable events](#), common cascading interactions and best practices for their management.

425 5 Conclusions

426 This study has characterised a post-wildfire multi-hazard cascade in a tropical montane catchment, demonstrating how the
427 burning of a pristine, fire-sensitive mountain ecosystem can initiate cascading hazards of exceptional intensity and persistence.
428 As fire regimes continue to shift to higher altitudes under climate change, there is an emerging risk of similar hazard cascades
429 for downstream communities in tropical mountain catchments worldwide- ([Mason et al., 2026](#)).

430
431 In Uganda's Rwenzori National Park, in the twelve years after a 2012 wildfire burned 31 km² of mature forest and peatland,
432 ten major floods with fluvial, debris or avulsion mechanisms occurred, with two debris floods requiring large-scale
433 humanitarian responses. Increased river discharge after the fire caused a 2.64-fold increase in erosion rates and increased the
434 probability of landslides, which have together driven a sevenfold increase in river channel width over nine years. Urban and
435 agricultural areas now face a real-time risk to public health due to the erosion and mass movement of 744,000 tonnes of copper-
436 cobalt solid tailings into the River Nyamwamba since 2014. This discrete escalation of hazards, interactions and impacts is
437 sustained by the slow recovery of vegetation poorly adapted to fire regimes, and multiple positive feedbacks between hazard
438 interactions.

439
440 The Rwenzori case highlights a need to recognise post-wildfire hazard cascades as a long-term risk in tropical mountain
441 environments, especially in newly fire-prone areas with no prior history of burning. High-income countries generally have
442 established post-fire risk assessment protocols, such as the Burned Area Emergency Response used in the USA (NICF, 2026),

443 and the Post Wildfire Natural Hazard Risk Analysis in British Colombia, Canada (Government of British Colombia, 2023).
444 Meanwhile, many low- and middle-income countries still lack standardised assessment procedures at the local or national
445 level. We recommend post-fire risk assessments and research, even for relatively small burn areas, when future fires occur in
446 previously unburned or fire sensitive mountain ecosystems. A better understanding of interactions between hazards identifies
447 intervention points, where interactions can be impeded through early actions that prevent ecosystem impacts from becoming
448 entrenched long-term. To this end, remediation of the burned zone should always be a priority to accelerate ecosystem recovery
449 and attenuate elevated runoff.

450

451 More monitoring and research of global case studies is needed to establish the prevalence and ~~intensitybehaviour~~ of tropical
452 mountain wildfire hazard cascades at emergent elevations, and best practices for their management. This study has additionally
453 underscored the value of integrating qualitative data and local knowledge into such studies. Interviews were critical to
454 identifying key hazard interactions that would not have been captured through physical or remote data alone. Interdisciplinary
455 research, through close partnerships between academic and local stakeholders, can improve collective visibility on this
456 emerging climate risk and accelerate the development of shared solutions.

457

458 **6 Data Availability**

459 The interview data is confidential according to ethical and data sharing restrictions. The GIS files are available on GitHub
460 (<https://github.com/will-veness/wildfires-uganda>) and will be available in Zenodo upon full publication.

461 **7 Competing Interests**

462 We declare no competing interests.

463 **8 Author Contributions**

464 William Veness: Writing – review & editing, Supervision, Writing – original draft, Visualization, Validation, Software, Resources, Project
465 administration, Methodology, Investigation, Funding acquisition, Formal analysis, Data curation, Conceptualization

466 Martha Day: Writing – review & editing, Writing – original draft, Visualization, Validation, Software, Resources, Methodology,
467 Investigation, Formal analysis, Data curation, Conceptualization

468 Anthony C. Ross: Writing – review & editing, Investigation, Data Curation, Validation

469 Yazidhi Bamutaze: Writing – review & editing, Funding acquisition, Data curation, Supervision, Investigation, Validation,
470 Conceptualization.

471 Jiayuan Han: Methodology, Investigation, Data Curation, Visualiazation, Software

472 Douglas Mulangwa: Project administration, Resources, Data curation, Investigation
473 Anthony Mwesigwa: Writing – review & editing, Project administration, Data curation, Investigation
474 Emmanuel Ntale: Project administration, Resources, Investigation
475 Callist Tindimugaya: Project administration, Resources, Methodology, Supervision, Conceptualization
476 Brian Guma: Project administration, Resources, Methodology, Investigation, Conceptualization, Supervision, Validation
477 Elisabeth Stephens: Writing – review & editing, Investigation, Project administration, Resources, Data Curation, Investigation, Validation
478 Wouter Buytaert: Writing – review & editing, Supervision, Methodology, Investigation, Project administration, Conceptualization,
479 Validation

480 **9 Acknowledgements**

481 We thank the Uganda Red Cross Society, the Ministry of Water and Environment, Kasese Municipality, and all local
482 collaborators and community members in Kasese District for their contributions to this research. We are grateful to the Uganda
483 Wildlife Authority and Rwenzori Trekking Services for facilitating access to the Rwenzori Mountains National Park. This
484 study was initiated through support from Imperial College London’s African Research Universities Alliance (ARUA)
485 partnership, which enabled collaboration with Makerere University. The Red Cross Red Crescent Climate Centre is also
486 gratefully acknowledged for its role in establishing the partnership with the Uganda Red Cross and the Ministry of Water and
487 Environment.

488 **10 References**

- 489 Abraham, M. R., & Susan, T. B. (2017). Water contamination with heavy metals and trace elements from Kilembe copper
490 mine and tailing sites in Western Uganda; implications for domestic water quality. *Chemosphere*, *169*, 281–287.
491 <https://doi.org/10.1016/j.chemosphere.2016.11.077>
492
493 Act Alliance. (2013). *ACT Alliance Preliminary Appeal UGA131: Flash Floods in Kasese, Uganda* [Data set].
494 <https://reliefweb.int/report/uganda/act-alliance-preliminary-appeal-uga131-flash-floods-kasese-uganda>
495 Act Alliance. (2020). *Uganda: Flood Emergency* (No. RRF No. 04/2020.) [Data set].
496
497 AghaKouchak, A., Chiang, F., Huning, L. S., Love, C. A., Mallakpour, I., Mazdiyasi, O., Moftakhari, H., Papalexioi, S. M.,
498 Ragno, E., & Sadegh, M. (2020). Climate Extremes and Compound Hazards in a Warming World. *Annual Review of Earth*
499 *and Planetary Sciences*, *48*(1), 519–548. <https://doi.org/10.1146/annurev-earth-071719-055228>
500
501 AghaKouchak, A., Huning, L. S., Chiang, F., Sadegh, M., Vahedifard, F., Mazdiyasi, O., Moftakhari, H., & Mallakpour, I.
502 (2018). How do natural hazards cascade to cause disasters? *Nature*, *561*(7724), 458–460. [https://doi.org/10.1038/d41586-018-](https://doi.org/10.1038/d41586-018-06783-6)
503 [06783-6](https://doi.org/10.1038/d41586-018-06783-6)
504
505 Ahmad, Z. U., Sakib, S., & Gang, D. D. (2016). Nonpoint Source Pollution. *Water Environment Research*, *88*(10), 1594–1619.
506 <https://doi.org/10.2175/106143016X14696400495497>
507
508 Arango-Carmona, M. I., Voit, P., Hürlimann, M., Aristizábal, E., & Korup, O. (2025). *Hillslope-Torrential Hazard Cascades*
509 *in Tropical Mountains*. Landslides and Debris Flows Hazards. <https://doi.org/10.5194/egusphere-2025-1698>

510 Asiimwe, W. (2014). Kasese Hit Fresh Floods. *New Vision*. <https://newvision.co.ug/news/1341922/kasese-hit-fresh-floods>
511
512 Belongia, M. F., Hammond Wagner, C., Seipp, K. Q., & Ajami, N. K. (2023). Building water resilience in the face of cascading
513 wildfire risks. *Science Advances*, 9(37), eadf9534. <https://doi.org/10.1126/sciadv.adf9534>
514
515 Bombino, G., D'Agostino, D., Marziliano, P. A., Pérez Cutillas, P., Praticò, S., Proto, A. R., Manti, L. M., Lofaro, G., &
516 Zimbone, S. M. (2024). A Nature-Based Approach Using Felled Burnt Logs to Enhance Forest Recovery Post-Fire and Reduce
517 Erosion Phenomena in the Mediterranean Area. *Land*, 13(2), 236. <https://doi.org/10.3390/land13020236>
518
519 Boyer, E. W., Wagenbrenner, J. W., & Zhang, L. (2022). Wildfire and hydrological processes. *Hydrological Processes*, 36(7),
520 e14640. <https://doi.org/10.1002/hyp.14640>
521
522 ~~British Geological Survey (2024) How to classify a landslide. British Geological Survey. Available at:~~
523 ~~<https://www.bgs.ac.uk/discovering-geology/earth-hazards/landslides/how-to-classify-a-landslide/#flows> (Accessed: 24 April~~
524 ~~2026).~~
525
526 Church, M., & Jakob, M. (2020). What Is a Debris Flood? *Water Resources Research*, 56(8), e2020WR027144.
527 <https://doi.org/10.1029/2020WR027144>
528
529 Coconino County Flood Control District. (no date). Alluvial Fan Stabilization Project. Coconino County, Arizona. Available
530 at: <https://www.coconino.az.gov/2407/Alluvial-Fan-Stabilization-Project> (Accessed: 12 April 2026).
531
532 Coalition for the Poudre River Watershed (CPRW). (no date). Low-Tech Process-Based Restoration. Available at:
533 <https://www.poudrewatershed.org/ltpbr> (Accessed: 12 April 2026).
534
535 Congedo, L. (2021). Semi-Automatic Classification Plugin: A Python tool for the download and processing of remote sensing
536 images in QGIS. *Journal of Open Source Software*, 6(64), 3172. <https://doi.org/10.21105/joss.03172>
537
538 Copernicus Climate Change Service (C3S). (2017). ERA5: Fifth generation of ECMWF atmospheric reanalyses of the global
539 climate [Dataset]. Copernicus Climate Change Service Climate Data Store (CDS). <https://doi.org/10.1002/qj.3803>
540
541 Costa, J.E. and Schuster, R.L. (1987) The formation and failure of natural dams. Open-File Report 87-392. Vancouver,
542 Washington: U.S. Geological Survey. Available at: <https://pubs.usgs.gov/of/1987/0392/report.pdf> (Accessed: 24 April 2026).
543
544 Creswell, J., W. (2009). *Research Design: Qualitative, Quantitative and Mixed Methods Approaches* (Third Edition).
545 https://www.ucg.ac.me/skladiste/blog_609332/objava_105202/fajlovi/Creswell.pdf
546
547 Cruden, D.M., Varnes, D.J. (1996) Landslide Types and Processes. Transportation Research Board, U.S. National Academy of
548 Sciences, Special Report, 247: 36-75
549
550 DeBano, L. F. (2000). The role of fire and soil heating on water repellency in wildland environments: A review. *Journal of*
551 *Hydrology*, 231–232, 195–206. [https://doi.org/10.1016/S0022-1694\(00\)00194-3](https://doi.org/10.1016/S0022-1694(00)00194-3)
552
553 Delforge, D., Wathelet, V., Below, R., Lanfredi Sofia, C., Tonnelier, M., van Loenhout, J. A. F., & Speybroeck, N. (2025).
554 *EM-DAT: The Emergency Events Database, International Journal of Disaster Risk Reduction* (No. 105509) [Data set].
555 <https://doi.org/10.1016/j.ijdrr.2025.105509.%202025>
556
557 DesInventar. (2025). *DesInventar Database* [Data set]. UNDRR. <https://www.desinventar.net/>
558

559 Doerr, S. H., Shakesby, R. A., & Walsh, R. P. D. (2000). Soil water repellency: Its causes, characteristics and hydro-
560 geomorphological significance. *Earth-Science Reviews*, 51(1–4), 33–65. [https://doi.org/10.1016/S0012-8252\(00\)00011-8](https://doi.org/10.1016/S0012-8252(00)00011-8)
561

562 Encalada, A. C., Flecker, A. S., Poff, N. L., Suárez, E., Herrera-R, G. A., Ríos-Touma, B., Jumani, S., Larson, E. I., &
563 Anderson, E. P. (2019). A global perspective on tropical montane rivers. *Science*, 365(6458), 1124–1129.
564 <https://doi.org/10.1126/science.aax1682>
565

566 European Environment Agency. (2025). *Nature-based solutions for fire-resilient European forests*. Publications Office of the
567 European Union. <https://doi.org/10.2800/8810870>

568 FAO. 2024. *Integrated fire management voluntary guidelines – Principles and strategic actions*. Second edition. Forestry
569 Working Paper, No. 41. Rome. <https://doi.org/10.4060/cd1090en>

570 FAO, & UNEP. (2020). *The State of the World's Forests 2020 [Table 6]*. FAO and UNEP. <https://doi.org/10.4060/ca8642en>
571 Flood List News. (2020a). Uganda – 8 Dead After More Floods in Kasese. *Flood List*. [https://floodlist.com/africa/uganda-](https://floodlist.com/africa/uganda-floods-kasese-may-2020)
572 [floods-kasese-may-2020](https://floodlist.com/africa/uganda-floods-kasese-may-2020)
573

574 FAO and UNEP. (2021). *Global assessment of soil pollution: Report*. <https://doi.org/10.4060/cb4894en>

575

576 Flood List News. (2020b). Uganda – Thousands Affected by Floods in Western Region. *Flood List*.
577 <https://floodlist.com/africa/uganda-thousands-affected-by-floods-in-western-region>
578

579 Galletta, A. (2020). *Mastering the Semi-Structured Interview and Beyond: From Research Design to Analysis and Publication*.
580 New York University Press. <https://doi.org/10.18574/nyu/9780814732939.001.0001>
581

582 Gearon, J., Martin, H. K., DeLisle, C., Barefoot, E. A., Mohrig, D., Paola, C., & Edmonds, D. A. (2024). Rules of River
583 Avulsion Supplementary Data Files (Version 0.0.2) [Data set]. Zenodo. <https://doi.org/10.5281/ZENODO.10338685>
584

585 Gill, J. C., & Malamud, B. D. (2016). Hazard interactions and interaction networks (cascades) within multi-
586 hazard methodologies. *Earth System Dynamics*, 7(3), 659–679. <https://doi.org/10.5194/esd-7-659-2016>
587

588 Google News. (2025). *Google News Search* [Data set]. Google News. [https://news.google.com/home?hl=en-](https://news.google.com/home?hl=en-GB&gl=GB&ceid=GB:en)
589 [GB&gl=GB&ceid=GB:en](https://news.google.com/home?hl=en-GB&gl=GB&ceid=GB:en)
590

591 Government of British Columbia. (2023). *Post wildfire natural hazard risk analysis*.
592 [https://www2.gov.bc.ca/gov/content/safety/wildfire-status/recovery/wildfire-land-based-recovery/post-wildfire-natural-](https://www2.gov.bc.ca/gov/content/safety/wildfire-status/recovery/wildfire-land-based-recovery/post-wildfire-natural-hazard-risk-analysis#PWFNHRA)
593 [hazard-risk-analysis#PWFNHRA](https://www2.gov.bc.ca/gov/content/safety/wildfire-status/recovery/wildfire-land-based-recovery/post-wildfire-natural-hazard-risk-analysis#PWFNHRA) Accessed 10th April 2026.
594

595 Guerriero, L., Tufano, R., Capozzi, V., Budillon, G., Di Muro, C., Esposito, L., Forte, G., Vitale, E., & Calcaterra, D. (2025).
596 A postwildfire debris flood in Gragnano, southern Italy, on September 11, 2024. *Landslides*, 22(6), 1923–1936.
597 <https://doi.org/10.1007/s10346-025-02509-8>
598

599 Haring, C. P., Altmann, G. L., Suedel, B. C., & Brown, S. W. (2021). Using Engineering With Nature® (EWN®) principles
600 to manage erosion of watersheds damaged by large-scale wildfires. *Integrated Environmental Assessment and Management*,
601 17(6), 1194–1202. <https://doi.org/10.1002/ieam.4453>

602 Hasanuzzaman, M., Islam, A., Bera, B., & Shit, P. K. (2024). Quantifying the riverbank erosion and accretion rate using DSAS
603 model study from the lower Ganga River, India. *Natural Hazards Research*, 4(4), 550–561.
604 <https://doi.org/10.1016/j.nhres.2023.12.015>

605 Hinzmann, A., Mölg, T., Braun, M., Cullen, N. J., Hardy, D. R., Kaser, G., & Prinz, R. (2024). Tropical glacier loss in East
606 Africa: Recent areal extents on Kilimanjaro, Mount Kenya, and in the Rwenzori Range from high-resolution remote sensing
607 data. *Environmental Research: Climate*, 3(1), 011003. <https://doi.org/10.1088/2752-5295/ad1fd7>

608 Hungr, O., Leroueil, S., & Picarelli, L. (2014). The Varnes classification of landslide types, an update. *Landslides*, 11(2), 167–
609 194. <https://doi.org/10.1007/s10346-013-0436-y>

610
611 Islam, A., & Guchhait, S. K. (2020). Characterizing cross-sectional morphology and channel inefficiency of lower Bhagirathi
612 River, India, in post-Farakka barrage condition. *Natural Hazards*, 103(3), 3803–3836. [https://doi.org/10.1007/s11069-020-
613 04156-9](https://doi.org/10.1007/s11069-020-04156-9)

614
615 Jacobs, L., Maes, J., Mertens, K., Sekajugo, J., Thiery, W., Van Lipzig, N., Poesen, J., Kervyn, M., & Dewitte, O. (2016).
616 Reconstruction of a flash flood event through a multi-hazard approach: Focus on the Rwenzori Mountains, Uganda. *Natural*
617 *Hazards*, 84(2), 851–876. <https://doi.org/10.1007/s11069-016-2458-y>

618
619 Jordan, P. (2016). Post-wildfire debris flows in southern British Columbia, Canada. *International Journal of Wildland Fire*,
620 25(3), 322. <https://doi.org/10.1071/WF14070>

621
622 Juma, B. (2016). Uganda – At Least 1,000 Displaced After Floods in Kasese and Kampala. *Flood List*.
623 <https://floodlist.com/africa/uganda-1000-displaced-floods-kasese-kampala>

624
625 Kappelle, M., Geuze, T., Leal, M. E., & Cleef, A. M. (1996). Successional age and forest structure in a Costa Rican upper
626 montane *Quercus* forest. *Journal of Tropical Ecology*, 12(5), 681–698. <https://doi.org/10.1017/S0266467400009871>

627
628 Kemter, M., Fischer, M., Luna, L. V., Schönfeldt, E., Vogel, J., Banerjee, A., Korup, O., & Thonicke, K. (2021). Cascading
629 Hazards in the Aftermath of Australia’s 2019/2020 Black Summer Wildfires. *Earth’s Future*, 9(3), e2020EF001884.
630 <https://doi.org/10.1029/2020EF001884>

631
632 Key, C. H., & Benson, N. C. (2006). *Landscape Assessment (LA)*.

633
634 Korup, O., and Schlunegger, F. (2007). Bedrock landsliding, river incision, and transience of geomorphic hillslope-channel
635 coupling: Evidence from inner gorges in the Swiss Alps. *Journal of Geophysical Research: Earth Surface*, 112(F3),
636 2006JF000710. <https://doi.org/10.1029/2006JF000710>

637
638 Lawler, D. M. (1993). The measurement of river bank erosion and lateral channel change: A review. *Earth Surface Processes*
639 *and Landforms*, 18(9), 777–821. <https://doi.org/10.1002/esp.3290180905>

640
641 Marengo, J. A., Cunha, A. P., Cuartas, L. A., Deusdará Leal, K. R., Broedel, E., Seluchi, M. E., Michelin, C. M., De Praga
642 Baião, C. F., Chuchón Angulo, E., Almeida, E. K., Kazmierczak, M. L., Mateus, N. P. A., Silva, R. C., & Bender, F. (2021).
643 Extreme Drought in the Brazilian Pantanal in 2019–2020: Characterization, Causes, and Impacts. *Frontiers in Water*, 3,
644 639204. <https://doi.org/10.3389/frwa.2021.639204>

645 Mason, A. L., Pereboom, E. M. B., Ivory, S. J., Vachula, R. S., Kelly, M. A., Nakileza, B., Russell, J. M. (2026). Twenty-first
646 century emergence of alpine fire in Central African mountains. *Nature*. 653, 746-751.

647
648 Maxar Technologies. (2025a). *Historical satellite imagery from March 2006 of Kilembe, Uganda via Google Earth Pro* [Data
649 set]. Google Earth Pro.

650
651 Maxar Technologies. (2025b). *Satellite imagery from 10th April 2023 of Kilembe, Uganda via Bing Maps* [Data set]. Bing
652 Maps. <https://www.bing.com/maps>

Field Code Changed

Formatted: Underline, Font color: Black

653
654 Mccaffrey, S. (2004). Thinking of Wildfire as a Natural Hazard. *Society & Natural Resources*, 17(6), 509–516.
655 <https://doi.org/10.1080/08941920490452445>
656
657 McGuire, L.A., Ebel, B.A., Rengers, F.K. *et al.* Fire effects on geomorphic processes. *Nat Rev Earth Environ* 5, 486–503
658 (2024). <https://doi.org/10.1038/s43017-024-00557-7>
659
660 McKee, T.B., Doesken, N.J. and Kleist, J. (1993) The Relationship of Drought Frequency and Duration to Time Scales. 8th
661 Conference on Applied Climatology, Anaheim, 17-22 January 1993, 179-184.
662
663 Mojtahed, R., Nunes, M. B., Martins, J. T., & Peng, A. (2014). *Equipping the Constructivist Researcher: The Combined use*
664 *of Semi-Structured Interviews and Decision-Making maps*. 12(2).
665
666 Moody, J. A., & Martin, D. A. (2001). Initial hydrologic and geomorphic response following a wildfire in the Colorado Front
667 Range. *Earth Surface Processes and Landforms*, 26(10), 1049–1070. <https://doi.org/10.1002/esp.253>
668
669 MoWE (2022). INTEGRATED WATER MANAGEMENT AND DEVELOPMENT PROJECT; IMPLEMENTATION OF
670 PRIORITY CATCHMENT MANAGEMENT MEASURES IN MIDSTREAM NYAMWAMBA (No. P163782). Uganda
671 Ministry of Water and Environment.
672
673 Muhamud, N. W., & Joyfred, A. (2015). Socio-Economic Factors Assessment Affecting the Adoption of Soil Conservation
674 Technologies on Rwenzori Mountain [Table 1]. *Indonesian Journal of Geography*, 47(1), 26. <https://doi.org/10.22146/ijg.6743>
675
676 Mukisa, W., Yatuha, J., Andama, M., & Kasangaki, A. (2020). Heavy metal pollution in the main rivers of Rwenzori Region,
677 Kasese District, South-Western Uganda. *Oct. Jour. Env. Res.* 8(3).
678
679 Mwesigye, A. R., & Lawrence, O. B. (2024). Trace Elements Contamination of Kilembe Copper Mine Catchment Soils in
680 Kasese District, Western Uganda. *Soil and Sediment Contamination: An International Journal*, 33(2), 232–243.
681 <https://doi.org/10.1080/15320383.2023.2195512>
682
683 Mwesigye, A. R., Young, S. D., Bailey, E. H., & Tumwebaze, S. B. (2016). Population exposure to trace elements in the
684 Kilembe copper mine area, Western Uganda: A pilot study. *Science of The Total Environment*, 573, 366–375.
685 <https://doi.org/10.1016/j.scitotenv.2016.08.125>
686
687 Mwonyera, A., Mbabazi, J., Muwanga, A., Ntale, M., & Kwetegyeka, J. (2014). Impact of the disused Kilembe mine pyrites
688 on the domestic water quality of Kasese town, western Uganda. *Caribbean Journal of Science and Technology (CJST)*, 2, 482–
689 495.
690
691 National Interagency Fire Centre (NICE). (2026). *Post Fire Recovery*. <https://www.nifc.gov/programs/post-fire-recovery>
692 (Accessed 10th April 2026).
693
694 New Vision. (2024). *Kasese PWDs bear the brunt of floods, landslides*. [https://www.newvision.co.ug/category/news/kasese-](https://www.newvision.co.ug/category/news/kasese-pwds-bear-the-brunt-of-floods-landslid-NV_188969)
695 [pwds-bear-the-brunt-of-floods-landslid-NV_188969](https://www.newvision.co.ug/category/news/kasese-pwds-bear-the-brunt-of-floods-landslid-NV_188969)
696
697 Nichter, K. A., Gilmore, T., Carbone, C., Sellers, B., Fairchild, M. P., & Preston, D. L. (2026). Ecological Characteristics of
698 Stream Reaches With and Without Low-Tech Process-Based Restoration in a Wildfire-Affected Catchment. *River Research*
699 *and Applications*, rra.70119. <https://doi.org/10.1002/rra.70119>
700
701 Norville, C., Ivory, S., Russell, J. M., Mason, A., Nakileza, B., & Miller, J. (2024, December). *Using charcoal to calibrate the*
702 *frequency of wildfire in the Rwenzori Mountains over the Holocene* [Conference poster]. AGU Fall Meeting 2024, Washington,
703 DC, United States.

- 701
702 [Oakley NS, Cheung DJ, Lindsay DN, Nash D. \(2025\) Insights from a 25-year database of post-fire debris flows in California. International Journal of Wildland Fire 34, WF25136. <https://doi.org/10.1071/WF25136>](#)
- 703
704
705 Obando-Cabrera, L., Díaz-Timoté, J. J., Bastarrika, A., Celis, N., & Hantson, S. (2025). The Paramo Fire Atlas: Quantifying
706 burned area and trends across the Tropical Andes. *Environmental Research Letters*, 20(5), 054019.
707 <https://doi.org/10.1088/1748-9326/adc8ba>
- 708
709 Okiror, S. (2020). 'People are desperate': Floods and rock slides devastate western Uganda. *The Guardian*.
710 [https://www.theguardian.com/global-development/2020/may/16/people-are-desperate-floods-and-rock-slides-devastate-](https://www.theguardian.com/global-development/2020/may/16/people-are-desperate-floods-and-rock-slides-devastate-western-uganda)
711 [western-uganda](https://www.theguardian.com/global-development/2020/may/16/people-are-desperate-floods-and-rock-slides-devastate-western-uganda)
- 712
713 Oliveras, I., Malhi, Y., Salinas, N., Huaman, V., Urquiaga-Flores, E., Kala-Mamani, J., Quintano-Loaiza, J. A., Cuba-Torres,
714 I., Lizarraga-Morales, N., & Román-Cuesta, R.-M. (2014). Changes in forest structure and composition after fire in tropical
715 montane cloud forests near the Andean treeline. *Plant Ecology & Diversity*, 7(1–2), 329–340.
716 <https://doi.org/10.1080/17550874.2013.816800>
- 717
718 Ometto, J. P., Kalaba, K., Anshari, G. Z., Chacon, N., Farrell, A., Halim, S. A., Neufeldt, H., & Sukumar, R. (2022). *Cross-*
719 *Chapter Paper 7: Tropical Forests. In: Climate Change 2022 – Impacts, Adaptation and Vulnerability: Working Group II*
720 *Contribution to the Sixth Assessment Report of the Intergovernmental Panel on Climate Change* (1st edn). Cambridge
721 University Press. <https://doi.org/10.1017/9781009325844.024>
- 722
723 Papaioannou, G., Alamanos, A., & Maris, F. (2023). Evaluating Post-Fire Erosion and Flood Protection Techniques: A
724 Narrative Review of Applications. *GeoHazards*, 4(4), 380–405. <https://doi.org/10.3390/geohazards4040022>
- 725
726 Paton, D. (2003). Disaster preparedness: A social-cognitive perspective. *Disaster Prevention and Management: An*
727 *International Journal*, 12(3), 210–216. <https://doi.org/10.1108/09653560310480686>
- 728
729 Patton, M. Q. (2014). *Qualitative Research & Evaluation Methods* (Fourth Edition). SAGE Publications, Inc.
730 <https://us.sagepub.com/en-us/nam/qualitative-research-evaluation-methods/book232962>
- 731
732 [Pierson, T. C. \(2005\). Hyperconcentrated flow – Transitional process between water flow and debris flow. In 'Debris flows and related phenomena'. \(Eds M Jakob, O Hungr\) pp. 159–202. \(Springer: Heidelberg, Germany\)](#)
- 733
734
735 Pivello, V. R., Vieira, I., Christianini, A. V., Ribeiro, D. B., Da Silva Menezes, L., Berlinck, C. N., Melo, F. P. L., Marengo,
736 J. A., Tornquist, C. G., Tomas, W. M., & Overbeck, G. E. (2021). Understanding Brazil's catastrophic fires: Causes,
737 consequences and policy needed to prevent future tragedies. *Perspectives in Ecology and Conservation*, 19(3), 233–255.
738 <https://doi.org/10.1016/j.pecon.2021.06.005>
- 739
740 ReliefWeb. (2024). Uganda—Floods (DG ECHO Partners, Uganda Red Cross, media) (ECHO Daily Flash of 10 September
741 2024)—Uganda. In *ReliefWeb*.
- 742
743 Rengers, F. K., McGuire, L. A., Oakley, N. S., Kean, J. W., Staley, D. M., & Tang, H. (2020). Landslides after wildfire:
744 Initiation, magnitude, and mobility. *Landslides*, 17(11), 2631–2641. <https://doi.org/10.1007/s10346-020-01506-3>
- 745
746 Ring, U. (2008). Extreme uplift of the Rwenzori Mountains in the East African Rift, Uganda: Structural framework and
747 possible role of glaciations. *Tectonics*, 27(4), 2007TC002176. <https://doi.org/10.1029/2007TC002176>
- 748
749 Robichaud, P. R., Lewis, S. A., Wagenbrenner, J. W., Ashmun, L. E., & Brown, R. E. (2013). Post-fire mulching for runoff
750 and erosion mitigation. *CATENA*, 105, 75–92. <https://doi.org/10.1016/j.catena.2012.11.015>

Formatted: Underline, Font color: Black

Field Code Changed

751 Rudoy, A. N. (2002). Glacier-dammed lakes and geological work of glacial superfloods in the Late Pleistocene, Southern
752 Siberia, Altai Mountains. *Quaternary International*, 87(1), 119–140. [https://doi.org/10.1016/S1040-6182\(01\)00066-0](https://doi.org/10.1016/S1040-6182(01)00066-0)

753 Saldana, J. (2021). *The Coding Manual for Qualitative Researchers*. [https://us.sagepub.com/en-us/nam/the-coding-manual-](https://us.sagepub.com/en-us/nam/the-coding-manual-for-qualitative-researchers/book273583)
754 [for-qualitative-researchers/book273583](https://us.sagepub.com/en-us/nam/the-coding-manual-for-qualitative-researchers/book273583)

755
756 Salinas, N., Cosio, E. G., Silman, M., Meir, P., Nottingham, A. T., Roman-Cuesta, R. M., & Malhi, Y. (2021). Editorial:
757 Tropical Montane Forests in a Changing Environment. *Frontiers in Plant Science*, 12, 712748.
758 <https://doi.org/10.3389/fpls.2021.712748>

759
760 Sanches Fernandes, L. F., Sampaio Pinto, A. A., Salgado Terêncio, D. P., Leal Pacheco, F. A., & Vitor Cortes, R. M. (2020).
761 Combination of Ecological Engineering Procedures Applied to Morphological Stabilization of Estuarine Banks after Dredging.
762 *Water*, 12(2), 391. <https://doi.org/10.3390/w12020391>

763
764 Sandwell, D., Anderson, D. L., & Wessel, P. (2005). Global tectonic maps. In G. R. Foulger, J. H. Natland, D. C. Presnall, &
765 D. L. Anderson, *Plates, plumes and paradigms*. Geological Society of America. <https://doi.org/10.1130/0-8137-2388-4.1>

766
767 Saunders, M., Lewis, P., & Thornhill, A. (2016). *Research methods for business students* (7th edition). Pearson.

768
769 Schenk, E. R., Wood, A., Haden, A., Baca, G., Fleishman, J., & Loverich, J. (2025). Post-wildfire sediment source and
770 transport modeling, empirical observations, and applied mitigation: An Arizona, USA, case study. *Natural Hazards and Earth*
771 *System Sciences*, 25(2), 727–745. <https://doi.org/10.5194/nhess-25-727-2025>

772
773 Scheper, A. C., Verweij, P. A., & Van Kuijk, M. (2021). Post-fire forest restoration in the humid tropics: A synthesis of
774 available strategies and knowledge gaps for effective restoration. *Science of The Total Environment*, 771, 144647.
775 <https://doi.org/10.1016/j.scitotenv.2020.144647>

776
777 Shakesby, R. A., & Doerr, S. H. (2006). Wildfire as a hydrological and geomorphological agent. *Earth-Science Reviews*, 74(3–
778 4), 269–307. <https://doi.org/10.1016/j.earscirev.2005.10.006>

779
780 Sklar, L. S., & Dietrich, W. E. (2001). Sediment and rock strength controls on river incision into bedrock. *Geology*, 29, 1087.
[https://doi.org/10.1130/0091-7613\(2001\)029%253C1087:SARSCO%253E2.0.CO;2](https://doi.org/10.1130/0091-7613(2001)029%253C1087:SARSCO%253E2.0.CO;2)

781
782 Slingerland, R., & Smith, N. D. (2004). RIVER AVULSIONS AND THEIR DEPOSITS. *Annual Review of Earth and*
783 *Planetary Sciences*, 32(1), 257–285. <https://doi.org/10.1146/annurev.earth.32.101802.120201>

784
785 Stock, J., & Dietrich, W. E. (2003). Valley incision by debris flows: Evidence of a topographic signature. *Water Resources*
Research, 39(4), 2001WR001057. <https://doi.org/10.1029/2001WR001057>

786
787 Stoof, C. R., Vervoort, R. W., Iwema, J., Van Den Elsen, E., Ferreira, A. J. D., & Ritsema, C. J. (2012). Hydrological response
788 of a small catchment burned by experimental fire. *Hydrology and Earth System Sciences*, 16(2), 267–285.
789 <https://doi.org/10.5194/hess-16-267-2012>

790
791 Swain, D. L., Prein, A. F., Abatzoglou, J. T., Albano, C. M., Brunner, M., Diffenbaugh, N. S., Singh, D., Skinner, C. B., &
792 Touma, D. (2025). Hydroclimate volatility on a warming Earth. *Nature Reviews Earth & Environment*, 6(1), 35–50.
793 <https://doi.org/10.1038/s43017-024-00624-z>

794
795 UNdata. (2026). UNdata Glossary: Nonpoint source pollution. Available at:
796 <https://data.un.org/Glossary.aspx?q=nonpoint+source+pollution> (Accessed: 24 April 2026)

- 797 UNDRR. (2025). Hazard Information Profiles. United Nations Office for Disaster Risk Reduction. Available at:
798 <https://www.preventionweb.net/drr-glossary/hips> (Accessed: 12 April 2026).
799
- 800 UNEP. (2022). *Spreading like wildfire—The rising threat of extraordinary landscape fires. A UNEP Rapid Response*
801 *Assessment*. United Nations Environment Programme.
802
- 803 UNESCO. (2012). State of conservation of World Heritage properties inscribed on the World Heritage List. WHC-
804 12/36.COM/7B. Paris: United Nations Educational, Scientific and Cultural Organization. Available at:
805 <https://whc.unesco.org/archive/2012/whc12-36com-7B-en.pdf> (Accessed: 12 April 2026).
806
- 807 UNESCO and WMO (Eds). (2012). *International glossary of hydrology: = Glossaire international d'hydrologie*. WMO.
808
- 809 Vahedifard, F., Abdollahi, M., Leshchinsky, B. A., Stark, T. D., Sadegh, M., & AghaKouchak, A. (2024). Interdependencies
810 Between Wildfire-Induced Alterations in Soil Properties, Near-Surface Processes, and Geohazards. *Earth and Space Science*,
811 11(2), e2023EA003498. <https://doi.org/10.1029/2023EA003498>
812
- 813 Veness, W. A., & Buytaert, W. (2025). Towards an evidence base for groundwater data investments. *Environmental Science*
814 *& Policy*, 164, 104014. <https://doi.org/10.1016/j.envsci.2025.104014>
815
- 816 Wesche, K., Miehe, G. and Kaeppli, M. (2000) 'The Significance of Fire for Afroalpine Ericaceous Vegetation', Mountain
817 Research and Development, 20(4), pp. 340–347. Available at: [https://doi.org/10.1659/0276-](https://doi.org/10.1659/0276-4741(2000)020[0340:TSOFFA]2.0.CO;2)
818 [4741\(2000\)020\[0340:TSOFFA\]2.0.CO;2](https://doi.org/10.1659/0276-4741(2000)020[0340:TSOFFA]2.0.CO;2)
819
- 820 Williams, D. J. (2015). Placing Soil Covers on Soft Mine Tailings. In *Ground Improvement Case Histories* (pp. 51–81).
821 Elsevier. <https://doi.org/10.1016/B978-0-08-100698-6.00002-7>
822
- 823 Wimberly, M. C., Wanyama, D., Doughty, R., Peiro, H., & Crowell, S. (2024). Increasing Fire Activity in African Tropical
824 Forests Is Associated With Deforestation and Climate Change. *Geophysical Research Letters*, 51(9), e2023GL106240.
825 <https://doi.org/10.1029/2023GL106240>
826
- 827 Wheaton, J. M., Bennett, S. N., Bouwes, N., Maestas, J. D., & Shahverdian, S. (2019). Low-Tech Process-Based Restoration
828 of Riverscapes: Design Manual. Version 1.0. <https://doi.org/10.13140/RG.2.2.19590.63049/2>

829 11 Appendices

830 Appendix A: 1-Month Standardised Precipitation Index Calculation for January 2012

831 ERA5 monthly averaged reanalysis total precipitation data was downloaded from 1974 – 2024 for the pixel covering to the
832 burned area (centroid coordinates: 0.4°N, 29.8°E; Copernicus Climate Change Service (C3S), 2017). This was processed in
833 MATLAB following McKee et al.'s (1993) method to determine the monthly-SPI for January 2012.
834

835 Appendix B: Eroded Tailings Volume Calculation

836 The average original height of the tailings was calculated to be 23 m, assumed to be flat across the original dammed area,
837 which was calculated (32945 m³) from historic satellite imagery.

838

839 This average height (23 m) was multiplied by the eroded footprint area (m²) to get a volume, then volumetric subtractions were
840 made to account for the originally sloped (55 degrees) walls of the tailings dam and the wedges of slumped material yet to be
841 eroded at the foot of the collapsed tailings escarpments. The volume of these wedges was calculated from the slope angle and
842 height of their triangular cross-section, multiplied by their width parallel to the eroded tailings escarpment.

843

844 The tonnage of eroded tailings was then calculated by multiplying their estimated volume by their assumed average dry density
845 (1.5 t/m³) based on standard values for copper-cobalt tailings (Williams, 2015).

846

847 **Appendix C: Semi-Structured Interview Template**

848 *Background*

- 849 ● What organisation do you represent?
- 850 ● What is your role?
- 851 ● What is your experience of hazards in the Rwenzori?

852

853 *Perceptions of changing hazard risk*

- 854 ● Do you feel the risk of hazards have changed (in the Nyamwamba catchment)? How?
- 855 ● If yes, why do you feel risk is changing?
- 856 ● Do you feel the river Nyamwamba/Mubuku/other rivers have changed?
- 857 ● If yes, why do you think this change has happened?

858

859 *Awareness and efficacy of existing management strategies*

- 860 ● What existing strategies are in place to manage hazard risk in the Rwenzori?
- 861 ● Do you feel these strategies are working?

862

863 *Potential alternative management strategies*

- 864 ● What strategies do you feel would better reduce hazard risk in the Rwenzori?
- 865 ● Why do you think these have not been implemented yet?
- 866 ● Do you feel nature-based solutions could be used to manage these hazards?

867

868

869

870

871 **Appendix D: The Multi-Hazard Cascade Interactions**

Table D1: Definitions of hazard terminology in this article from the 2025 Hazard Information Profiles (HIPs; UNDRR, 2025).

*Both avulsion flooding and debris flooding are profiled under Flooding - MH0600 (UNDRR, 2025) however further distinction using key references between these types of flooding is important here for understanding the hazard cascade and its interactions.

Formatted Table

Hazard	HIPs 2025 Definition	HIP 2025 Identifier	Primary Source(s)
Wildfire	Any unplanned and uncontrolled vegetation fire that, regardless of ignition source, may negatively affect social, economic or environmental values, and require suppression response or other action according to agency policy (FAO, 2024).	EN0205	FAO (2024)
Runoff Pollution	Nonpoint sources of pollution refer to pollution that does not have a single point of origin or has not been introduced into a receiving freshwater or maritime environment from a specific outlet. The pollutants are generally carried off from the land by agricultural runoff, urban stormwater, atmospheric deposition or subaqueous groundwater discharges. The most common categories of nonpoint pollution are agriculture, forestry, urban areas, mining, construction, dams and channels, land disposal and saltwater intrusion.	EN0106	UNdata (2026) Admad, Sakib and Gang (2016)
Fluvial Flooding	Overflowing by water of the normal confines of a watercourse or other body of water (WMO, 2012).	MH0604	UNESCO and WMO (2012)
*Avulsion Flooding	River avulsions are an abrupt change in a rivers course to establish a new river channel. These are natural phenomena as the river migrates across the floodplain but can result in devastating avulsion floods. Whilst their mechanism is not yet fully understood, they are considered to occur when sediment depositions downstream of the avulsion location cause the existing channel to become unfavourable and so the channel switches to a route with a more efficient flow pathway (Singerland and Smith, 2004; Gearon et al., 2024).	MH0600	Singerland and Smith (2004) Gearon et al. (2024)
River Erosion and Accretion	River erosion is the removal of material from the banks and beds of rivers and streams (Lawler, 1993). River accretion is the formation of new land such as channel bars, sandbanks and deltas by sedimentation or changing river flow (after Islam and Guchhait, 2020 and Hasanuzzaman et al., 2024).	GH0404	Lawler (1993) Hasanuzzaman et al. (2024)

			Islam and Guchhait (2020)
Debris Flows	<p>Flows are gravitational mass movements down a slope in the form of a fluid. Flows often leave behind a distinctive, fan-shaped deposit where the landslide material has stopped moving (British Geological Survey 2024). Sub-categories of flows may be defined by the type and proportion of material (e.g., soil, debris, or earth) and the velocity of the mass movement, Cruden and Varnes, 1996; Hungr, Leroueil and Picarelli, 2014).</p> <p><u>Debris flows are rapid, gravity-driven flows of poorly sorted material in which water and sediment form a dense slurry, typically with sediment concentrations exceeding 50% by volume (Rengers et al., 2020; Pierson, 2005). This distinguishes them from hyperconcentrated flows (approximately 20-60% sediment by volume) and water-dominated floods (below approximately 10% sediment by volume) in which flow behaviour is primarily controlled by water instead of the entrained sediment (Pierson, 2005). Debris flows behave like wet concrete, capable of holding gravel in suspension at low velocities, and transporting large boulders and woody debris at high velocities (Pierson, 2005). Due to their density and momentum, they are generally more destructive than floods or debris floods and can cause catastrophic damage through impact and burial (Pierson, 2005). Post-fire debris flows are fast moving slurries of soil, ash, rocks, burned vegetation and water, typically triggered by short-duration, high-intensity rainfall in the first few years following a fire (Oakley et al., 2025; Rengers et al., 2020).</u></p>	GH0303	<p>British Geological Survey (2024)</p> <p>Cruden and Varnes (1996)</p> <p>Hungr, Leroueil and Picarelli (2014)</p> <p>Rengers et al. (2020)</p> <p>Pierson (2005)</p> <p>Oakley et al. (2025)</p>
*Debris Flooding	<p>Debris floods are 'very rapid flow of water, heavily charged with debris, in a steep channel...' in which 'the streambed may be destabilized' (Hungr, Leroueil and Picarelli, 2014) resulting in massive sediment transport over large distances (Church and Jakobs, 2020).</p> <p><u>Crucially, flow behaviour in a debris flood is still controlled by water rather than the entrained sediment (Pierson, 2005), and peak discharge remains comparable in order of magnitude to that of a water-dominated flood.</u></p>	MH0600	<p>Hungr, Leroueil and Picarelli (2014)</p> <p>Church and Jakobs (2020)</p> <p>Pierson (2005)</p>
Landslide**	<p>A gravitational mass movement ('landslide') is the downslope movement of soil, rock and organic materials under the effects of gravity, which occurs when the gravitational driving forces exceed the frictional resistance of the material resisting on the slope. Such movements may be terrestrial or submarine (GH0306) (Cruden and Varnes, 1996).</p>	GH0300	Cruden and Varnes (1996)

**Here, we define landslides as those connected to the river system.

Heavy Metal Pollution	Heavy metals are metallic trace elements with either high relative atomic weights or occurring in materials with high densities. Trace Elements is the term used for elements that are generally found in soil at low concentrations. Trace elements can become contaminants when their concentrations significantly exceed natural levels due to anthropogenic activities, such as industrial processes, mining, agriculture, and waste disposal. These contaminants can accumulate in soil, water, and biota, potentially causing adverse effects on ecosystems and human health.	CH0100	FAO and UNEP (2021)
------------------------------	---	--------	---------------------

Table D2: Description of the hazard interactions in Fig. 2 and supporting evidence.

#	Initiating Hazard	Affected Hazard	Interaction Description	Evidence
1	Wildfire	Runoff pollution	Increased probability. Burning of soils and vegetation cover increased their erosion and runoff to the river channel. This hazard is also catalysed by higher rates of erosion increasing the delivery of soil, ash and peat to the river.	Four interview respondents describing increased turbidity immediately after the wildfire and during high flows, with a smell "like methane" [M1, M2, R1, G1].
2	Wildfire	Fluvial flood	Increased probability. Burning of vegetation has reduced interception and root uptake of precipitation, increasing surface runoff to the channel. This has increased peak discharges at reduced lag times following peak rainfall events. The burning and erosion of mature soils has also reduced their infiltration and storage capacities, therefore increasing runoff.	Humanitarian data of 10 flood events since 2012 exceeding the impacts of any documented flood in the 12 years prior (Table 1). Interviewee accounts [M1, M2, G1, G2, R1], e.g. <i>"the burning is the reason we are now having the floods annually... we know how useful wetland vegetation is in controlling floods, releasing water slowly"</i> [G1].
3	Wildfire	River channel erosion	Increased probability. Wildfire's burning of vegetation and erosion of soil has increased runoff, peak river discharge, and therefore the erosive power of the river. Initial erosion and mass movement also exposed riverbanks, which is increasing the probability of (and catalysing) further erosion in a positive feedback process.	GIS analysis calculating an erosion rate increase by a factor of 2.64 due to the wildfire (Fig. 4). Photographs of exposed riverbanks within wildfire affected areas (Fig. 3c and Appendix F).
4	Wildfire	Debris flood	Increased probability. Wildfire has increased peak river discharge by the burning of vegetation and soil which modulate discharge. It has also increased sediment generation through augmented erosion and mass	Two interview respondents explain and show camera footage of 2013 and 2020 debris floods, described as unprecedented before the fire [M1, R1] (Table 1). Jacob's et al.'s (2016) reconstruction of debris flood during the May 2013 flood.

Formatted Table

			movement, improving the conditions for debris flood development.	Field photographs of boulder deposition on the delta and distal flood plain (Appendix G).
7	Fluvial flood	Fluvial flood	Increased probability. Fluvial floods damage engineered flood defences, increasing the probability of future breaches.	Photos of damaged flood defences (Appendix H).
8	Fluvial flood	River channel erosion	Triggering. Higher flow velocities and turbulence during fluvial floods exert shear stress, abrasion and hydraulic action to erode riverbanks.	GIS analysis shows the years of highest erosion occurred in 2013 and 2020, the years of the largest debris and fluvial floods [M1, R1] (Fig. 4).
6*	Fluvial flood	Runoff pollution	Triggering. Fluvial floods transport materials across the urban and agricultural landscape. If pollutants are present, this results in a runoff pollution event. *This is also true of avulsion floods and debris floods	Respondents describe post-flood contamination of urban and agricultural landscapes [M1, M2]. Field photographs of contaminant transport into urban areas (Appendix L, Fig. L1).
9	River channel erosion and accretion	Fluvial flood	Increased probability. Eroded material fills and reduces the channel's carrying capacity for discharge. Erosion has also relocated active channels closer to residential areas.	Change in river morphology to a sediment-laden braided system indicating increased deposition and channel switching (Fig. 4b).
10	River channel erosion and accretion	Landslide	Triggering. Lateral and vertical erosion of riverbanks undercuts and destabilises hillslopes, increasing local shear stresses to failure.	Jacobs et al. (2016) map 14 landslides triggered by scour and bank failure from river erosion.
11	River channel erosion and accretion	River channel erosion	Increased probability. Erosion of banks exposes steep, unstable riverbanks to further erosion.	Photos of erosional riverbanks incising into hillslopes at multiple sites (Appendix F). Interviewee descriptions [G1, G2, M1]
12	River channel erosion and accretion	Heavy metal pollution	Triggering. River erosion has breached the main 15 Mt solid Co-Cu Kilembe Mines tailings deposit and other smaller deposits within the town.	Satellite images and field photographs (Fig. 4) show erosive riverbanks and new channels within the original tailings area. Field observations of downstream deposition of tailings and iron precipitates (Appendix E). Four respondents consider waste deposition a major concern for public health and a potential cause of vegetation death on the riverbanks [M2, W1, G2, R1].
14	River channel erosion and accretion	Avulsion flood	Triggering. Increased erosion of riverbanks causes channel-switching and subsequent avulsion floods.	Humanitarian data and interview respondents [M1, M2] describing the 22nd May 2024 avulsion flood impacting Kasese town (Table 1).
13	River channel erosion and accretion	Avulsion flood	Increased probability. Higher rates of upstream erosion increase downstream deposition in channel bars, diverting flow towards riverbanks.	Interview respondents [M1, M2] describing the 22nd May 2024 avulsion flood impacting Kasese town (Table 1) and the increased rate of deposition that has raised dredging and channel clearance costs since the 2012 wildfire [M1, M2, R1].
17	River channel erosion and accretion	Debris flood	Increased probability. Erosion provides additional sediment that improves the probability of debris flood formation.	GIS analysis of increased channel area and width (Fig. 3) filled with coarse sediment in a braided system (Appendix K).

				Two respondents describe debris floods as unprecedented before the fire [M1, R1].
15	River channel erosion and accretion	River channel erosion	Increased probability. Sediment deposition narrows the active channel cross-section, increasing the flow velocity and erosive potential driving further channel erosion.	Interview respondents describing sediment erosion and accretion processes in river channel [M1, M2, R1, G1, G2]. GIS analysis of increased channel area and width (Fig. 3) filled with coarse sediment in a braided system (Appendix K).
16	River channel erosion and accretion	River channel accretion	Increased probability. Sediment deposition narrows the active channel cross-section, increasing the flow velocity and erosive potential driving further channel erosion (#15). The eroded material replenishes the sediment supply available for sediment deposition (#16), sustaining this cycle.	Interview respondents describing sediment erosion and accretion processes in river channel [M1, M2, R1, G1, G2]. GIS analysis of increased channel area and width (Fig. 3) filled with coarse sediment in a braided system (Appendix K).
20	Debris flood	Debris flood	Increased probability. Debris floods damage engineered flood defences, increasing the probability of future breaches.	Photos of damaged flood defences (Appendix H).
18	Debris flood	River channel erosion	Triggering. Debris floods have high erosive power (Church & Jakob, 2020).	GIS analysis shows the years of highest erosion occurred in 2013 and 2020, the years of the largest debris and fluvial floods [M1, R1] (Appendix K).
19	Debris flood	River channel accretion	Triggering. Debris floods deliver mobilized sediment directly into the river channel, promoting accretion and progressively altering channel geometry over time.	Interview respondents describing the increase in channel sediment deposition following debris flood events [M1; M2; R1].
24	Landslide	Heavy metal pollution	Triggering. Rotational slumping of the soft, unconsolidated tailings into the River Nyamwamba causes heavy metal contamination of water and sediment.	Satellite images and field observations (Appendix K) show rotational slump scars throughout the affected tailings. Four respondents consider waste deposition a major concern for public health and a potential cause of vegetation death on the riverbanks [M2, W1, G2, R1].
23	Landslide	River channel erosion	Increased probability. Landslides increase sediment load and the subsequent erosive power of the river through abrasion.	Interview respondents describing the increase in channel sediment deposition following landslides [R1; M1; M2; I1; G2]. Field photographs of slump scars on riverbanks (Appendix I). Analysis by Jacobs et al. (2016) showing landslides directly entering the river system.
22	Landslide	River channel accretion	Increased probability. Landslides add increase sediment load, accelerating accretion and lateral erosion by diverting flow to the riverbanks.	Interview respondents describing the increase in channel sediment deposition following landslides [R1; M1; M2; I1; G2]. Field photographs of slump scars on riverbanks (Appendix I). Analysis by Jacobs et al. (2016) showing landslides directly entering the river system.

21	Landslide	Fluvial flood	<p>Increased probability. Landslide material fills and reduces the channel's carrying capacity for discharge.</p> <p>Landslides also increase the probability of fluvial (and debris) flooding through temporary damming and bursting mechanisms that create surges of discharge.</p>	<p>Jacobs et al. (2016) mapped 29 landslides during the May 2013 flood that directly entered the River Nyamwamba.</p> <p>Five respondents describe a mechanism of temporary landslide damming and bursting "in the space of a few minutes" [M1] during peak rainfall events in the upper-catchment [G1, M1, M2, R1, W1].</p>
5	Runoff pollution	River channel accretion	<p>Increased probability. Runoff pollution from the burned area transports elevated loads of fine sediment and contaminants into the river channel. Increased sediment supply promotes channel accretion as the excess sediment load settles into the river channel.</p>	<p>Four interview respondents describing increased turbidity immediately after the wildfire and during high flows, with a smell "like methane" [M1, M2, R1, G1].</p> <p>GIS analysis of increased channel area and width (Fig. 3) filled with coarse sediment in a braided system (Appendix K).</p>

875
876
877



879

880

Figure E1: Acid mine drainage at location 0.18599N, 30.01951E, 25 July 2024.



881
882 **Figure E2: Acid mine drainage at location 0.19879N, 30.01139E, 3 August 2024.**



883
884

Figure E3: Tailings sedimentation in the Nyamwamba channel, 0.18652N, 30.01986E, 25 July 2024.

885 **Appendix F: Exposed Riverbank Photographs**



886
887 **Figure F1: Riverbank exposure at 0.29291N, 29.93596E – 28 July 2024.**
888



889
890 **Figure F2: Riverbank style erosion of house foundations in Kilembe, 0.20603N, 30.00822E – 24 July 2024.**

891
892
893
894
895
896
897
898
899
900
901



902
903 **Figure F3: Riverbank at 0.23742N, 23.97568E – 1 August 2024.**



904
905 **Figure F4: Riverbank at 0.23715N, 29.97601E – 1 August 2024.**
906

907 **Appendix G: Flood Plain Boulder Deposition Photographs**



908
909

Figure G1: 0.20285N, 30.00908E - 7 June 2023.



910
911
912

Figure G2: 0.19528N, 30.01544E - 25 July 2024.

913 **Appendix H: Damaged Flood Defences Photographs**



914
915 **Figure H1: 0.18981N, 30.07408E, 26 July 2024 (damaged bamboo nature-based solution).**

916



917
918

Figure H2: 0.21387N, 30.00558E, 7 June 2023 (damaged gabions).

919 **Appendix I: Landslide Talus Entering the River Photographs**



920
921 **Figure II: 0.29291N, 29.93596E – 28 July 2024.**



922
923 **Figure I2: Landslide scar at 0.23758N, 29.97570E – 1 August 2024.**
924
925
926
927
928
929
930
931
932

933 **Appendix J: Lower Course Deposition of Solid Mine Tailings Photographs**



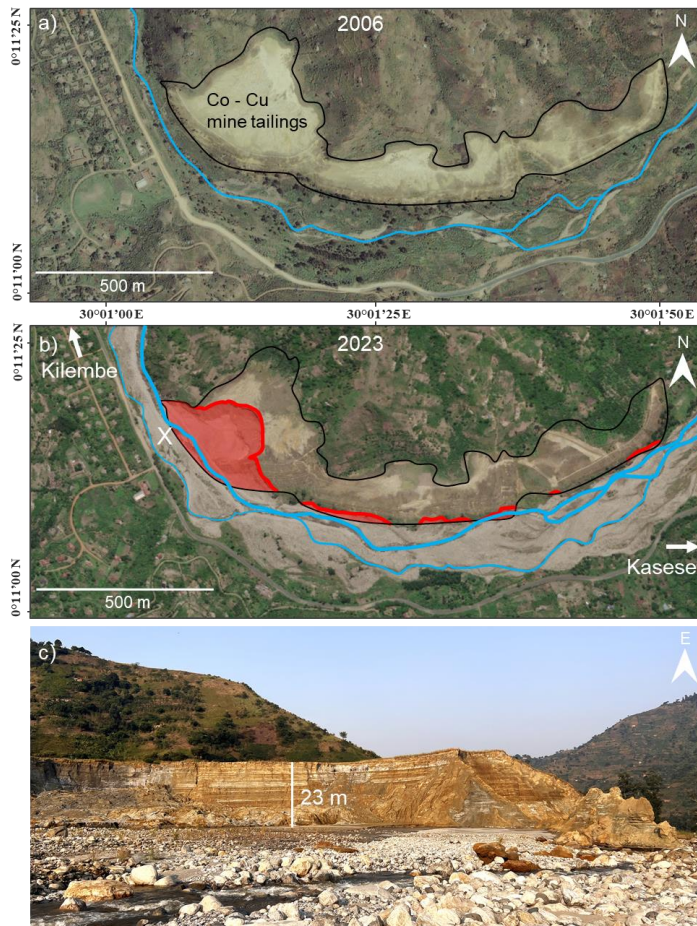
934
935 **Figure J1: Deposition and acid mine drainage downstream of Kilembe Mines 0.19385N, 30.082355 E, 26 July 2024.**



936
937

Figure J2: Acid mine drainage from deposited solid tailings at location adjacent to Kasese town, 26 July 2024.

938 **Appendix K: Kilembe Mines Co-Cu Tailings Erosion**



939

940

941

942

943

944

Figure K1 – a) Kilembe Mines tailings on 24th March 2006 (Maxar Technologies, 2024a); b) the same location on 10th Apr 2023 (Maxar Technologies, 2024b) where an estimated 744,000 tonnes of solid waste have eroded into the river. The black polygon outlines the original surface area of mine tailings, and the red polygon shows the area partly or fully eroded; c) photograph of a section of the eroded tailings taken in July 2024 at position X (b), facing east towards Kasese town.

945 **Appendix L: Post-flood photos from September 2024 flood event**



946
947 **Figure L1: Photograph following flooding in Kasese town evidencing the inundation level and post-flood ground**
948 **contamination. Photograph provided by the Ministry of Water and Environment.**

949 **Appendix M: Management Strategies and their Evaluation**

950 The disaster risk management (DRM) strategies in Table L1 have been implemented in the Nyamwamba catchment since the
951 May 2013 floods. Whilst relocation of communities experiencing near-annual flooding is considered desirable for mitigating
952 their flood risk [M1, M2, N1], residents have opposed relocation due to existing community and land ties, lower living costs
953 on flood plain and a lack of economic opportunity in areas proposed for relocation [M1, G2, N1]. Instead, therefore, strategies
954 have focussed on protecting existing communities and informal settlements on the flood plain with hard engineering,
955 community-centred and nature-based solutions (Table L1).

956
957 **Table M1 – Summary of disaster risk reduction strategies in Kasese Districts observed during field reconnaissance and described**
958 **by interview respondents.**
959

Strategy	Description	Evaluation	
Hard Engineering	Gabions (Figure M1a)	Installed in phases along a 2-3 km alongside Kilembe town to mitigate flooding and river channel switching.	"The Gabions have failed, they're very weak" [R1]. Damaged by minor flood events (Appendix H), and they have failed to prevent channel overtopping into Kilembe Town during the 22 nd May 2024 flood [M2].
	Channelisation (Figure M1b)	A short 500 m channelised section of channel downstream from Kilembe, using concrete to ensure the stability of the road-bridge providing the only access route to Kilembe town.	"what they have done [at the bridge] is perfect...the narrow section never gets clogged up so the rocks pass through" [R1]. The solution has been positively received [R1, R2], but it is considered expensive, and river may switch channels if extended [M2].
	Dredging	5 km of channel is desilted (boulders are broken down and removed from the active water channels to the banks) in an irregular regime, typically funded after major floods such as those in 2013 and 2020 [M1, M2].	It costs US\$4.5 million to clear 5 km of the channel and it needs to be performed annually to maintain a cleared channel [M2]. Residents recall successful desilting by a Canadian mining company until the 1971, so it is a positively viewed activity [G1, G2, W1] but may not be economically sustainable with the currently increased sediment flux of the river [M1]. It does not take place far enough upstream of Kilembe where debris floods generate [R1, M2].
Community-Centred Solutions	Flood Early Warning Systems (Figure M1c)	Communities of Kilembe, Kasese and Mubuku given early warnings through the Ugandan Red Cross and the Ugandan Ministry of Water and Environment (MoWE) following alerts of high rainfall.	"with early warning systems, less people are dying... people are more informed with better risk communication" [N1]. However, difficulties monitoring water levels due to high sediment loads and channel switching leaves early warning dependent on rainfall forecasts that are low-confidence in a convectional mountainous region [M2]. Expansion requires greater hydrological monitoring for more accurate, confident and timely warnings [N1, M2].
	Resident Relocation	Relocation of displaced households from Kilembe and riverbanks to the Kasese lowlands, using emergency response funding following major 2013 and 2020 flood events [N1, M1]. Matched with investment to support alternative livelihoods independent of the river such as bee keeping [M1].	In most cases, residents have refused to relocate and are building informal homes [M1]. There is a need for expansion of livelihood incentives and longer-term support investments for their setup [G2]. High flood risk areas offer low-cost land, economic opportunities, free water from the river and many have attachment to lands from family history, mountain livelihoods and lived experience [N1].
	Participatory Desilting	Pilot project training individuals to convert river boulders into crafts, such as granite wash-basins to be sold to safari lodges and tourists.	It is not being completed at a scale that significantly impacts flood risk [M1], but it has been shown to successfully supplement family incomes (Ugandan Ministry of Water

Formatted Table

			and Environment (MoWE), 2022). It requires longer-term investment and a plan for expansion and greater access to the market [N1, M1].
Nature-based Solutions (NbS)	Riverbank Stabilisation (Figure M1d)	As part of a 2021 World Bank funded project (MoWE, 2022), a 10 km length of the Nyamwamba riverbanks have been planted with 30 m thick vegetation buffers to mitigate further lateral erosion. Seedlings planted included 35,000 Asper bamboo, 2,000 mango and 4,000 Mahogany, situated within a fenced zone to deter trespassing, logging, theft and interference by animals (MoWE, 2022).	An existing pilot in Mubuku has demonstrated 20 years of successful bank stabilisation [M1], however 2021 Nyamwamba planting has faced challenges of droughts, floods, termites [W1], death of seedlings due to heavy metal contamination by mine tailings, logging, and reluctant participation by some land owners. Rapid initial growth in patches require long term monitoring and evaluation, but bamboo planting is perceived as the most promising solution for landslide and erosion mitigation in the wildfire-affected zone and around the mine tailings [R1, M1, M2, I1, I2, W1]
	Soil and Water Conservation	Awareness raised among 1,420 land owners of methods available to reduce soil erosion and runoff. 750 were trained to implement the intervention and provided equipment, with 211 hectares of land modified by the addition of trenches and hedges in 2021-2022 (MoWE, 2022). Households encouraged to harvest rainwater instead of drinking from the river.	“there was actually a gentleman that implemented it on his own land, without us telling him to.” Need for more land-owner co-operatives to share trainings, to share risk of failed implementation following land conversion, and to share tedious workloads [G2]. Rainwater harvesting reduces runoff, soil erosion on small plots and decreases heavy metal consumption from river water [M2, G2].
	Afforestation and Regrading of Hillslopes	825 hectares afforested through reforestation and agroforestry in the mid-catchment to reduce landslides, soil erosion and runoff to the river (MoWE, 2022).	Soil-water conservation trenches and soil-stabilising species increased coffee yields [F1]. Some respondents criticised soil-water conservation and afforestation efforts for focussing on the mid-catchment, when “99%” of the sediment and discharge generation is taking place in the burned national park area upstream [R1, I2]. “Until we stabilise those areas [upstream] we will have these problems” [I2].

960

961

962

963

964

965

966

967

For hard engineering strategies, respondents believe that gabions are too weak to sustainably channelise the river [R1, M2] (Figure M1a), whereas there is demand for the successful concrete channelisation to be extended beyond Kilembe town centre [R1, R2, M2] (Figure M1b). Channel dredging is perceived to be a critical activity, not because of successful implementations since 2013, but due to successful historic programmes of dredging by mining companies when Kilembe mines was operational in the 1960s [G1, G2, W1, R1, M2]. For all hard engineering approaches, there is concern of an unsustainably high cost of maintenance, given the elevated rate of discharge, erosion and sediment generation in the Nyamwamba river [M1, M2].

968 Flood early warning systems piloted in Kilembe and Kasese using 2 local rain gauges and water level sensors have faced
969 challenges of continuous automated data collection in hard-to-reach upstream locations, however, sharing of information
970 between authorities and community representatives via Whatsapp has successfully coordinated evacuations following high
971 flows and rapid dispatches of emergency respondents [N1]. A 2023 installation of a camera 5 km upstream of Kilembe, capable
972 of international photo and video transmission at 1-minute intervals (Figure M1c), is considered a useful supplementary dataset
973 for a more detailed interpretation by those with lived experience and indigenous knowledge of the river [N1, M2]. For rivers
974 with a debris-flow model of flooding, setting qualitative thresholds of perceived flood severity from imagery may have more
975 local predictive value than water levels in channels where channel location and roughness change frequently [M2].

976
977 A project funded by the World Bank and implemented by the Ugandan Ministry of Water and Environment (MoWE) in 2021
978 – 2022 has installed a range of nature-based (NbS) and community-centred solutions (MoWE, 2022). The NbS of riverbank
979 stabilisation in Kasese is considered especially promising [R1, R3, W1, M1, M2], using 35,000 asper bamboo seedlings and
980 other economic crops in buffer zones on the mid-catchment riverbanks to prevent erosion. Despite challenges with drought,
981 flooding, termites and metal-contaminated soils during the early implementation [W1, M2, G2], a previous project successfully
982 stabilising the Mubuku riverbanks for 20 years [M1] and observations of stable bamboo forests in the upper catchment [R1]
983 provide optimism for the project. Respondents are more critical of other parts of the project, including soil-water conservation
984 and participatory desilting of the river (Table L1), for focussing on the mid-catchment around Kasese town, when discharge
985 and sediment generation is taking place higher in the mountains [R1, I2].

986
987

“the assumptions made are well off beat; “99% of the water is coming from the park” – R1



988
989
990
991
992
993

Figure M1 – Photographs taken during June 2023 field reconnaissance: a) collapsed gabions adjacent to Kilembe town (for scale: 8 m channel width); b) channelisation using concrete embankments in Kilembe town centre (10 m channel width under bridge); c) photo from a camera transmitting photos at 1-minute intervals 5 km upstream of Kilembe town centre for flood early warning; d) riverbank stabilisation adjacent to Kasese town including asper bamboo (4 m fencepost spacing).

994 Notably, there have been no DRR interventions so far in the wildfire affected area of the upper catchment, and no active
995 mitigation of mine tailing erosion into the river Nyamwamba. In both cases, a low awareness of their impacts has inhibited
996 action [M2, R1, W1, G2]. 7 of 12 interview respondents did not mention the 2012 wildfire when asked to describe factors
997 affecting local flood risk, and only one small-scale academic study has assessed water quality in the Nyamwamba since large-
998 scale erosion began in 2015 (Mukisa et al., 2020). Of the respondents aware of the wildfire [R1, W1, M1, M2, G2] and water
999 quality problems [M1, M2, G1, G2] in the Nyamwamba catchment, all recommend restoration of the wildfire-affected area
1000 and urgent mitigation of further erosion into the river.